Microwave-assisted dry reforming of methane for syngas production: a review

T. T. Phuong Pham, Kyoung Ro, Lyufei Chen, Devinder Mahajan, Tan Ji Siang, U. Ashik, Jun-Ichiro Hayashi, Doan Pham Minh, Dai-Viet Vo

Microwave-assisted dry reforming of methane for syngas production: a review

T. T. Phuong Pham[1,2] · Kyoung S. Ro[3] · Lyufei Chen[4] · Devinder Mahajan[4] · Tan Ji Siang[5] · U. P. M. Ashik[6] · Jun-ichiro Hayashi[6,7] · Doan Pham Minh[8,9] · Dai-Viet N. Vo[10]

Abstract

Abatement of emissions of greenhouse gases such as methane and carbon dioxide is crucial to reduce global warming. For that, dry reforming of methane allows to convert methane and carbon dioxide into useful synthesis gas, named 'syngas', a gas mixture rich in hydrogen and carbon monoxide. However, this process requires high temperatures of about 900 °C to activate methane and carbon dioxide because dry reforming of methane reaction is highly endothermic. Therefore, a solid catalyst with appropriate thermal properties is needed for the reaction. As a consequence, efficient heating of the reactor is required to control heat transfer and optimize energy consumption. Microwave-assisted dry reforming of methane thus appears as a promising alternative to conventional heating. Here we review the recent research on microwave-assisted dry reforming of methane. We present thermodynamical aspects of the dry reforming of methane, and basics of microwave heating and apparatus. We analyse reformers that use microwave heating. Catalysts used in a microwave-assisted reformer are presented and compared with reactors using conventional heating. Finally, the energy balance is discussed.

Keyword Dry reforming of methane · Syngas · Microwave-assisted · Catalyst · Energy balance

Abbreviations

BMR	Bi-reforming of methane
btoe	Billion tonnes oil equivalent
CNTs-HPCFs	Carbon nanotubes-hollow porous carbon fibres
CQ	Metallurgical coke
C/MR	Catalyst and microwave receptor
DRM	Dry reforming of methane
eFe	Steel-making slag
FTIR	Fourier transform infrared spectroscopy
IEA	International energy agency
Microwave-assisted DRM	Microwave-assisted dry reforming of methane
MAE	Microwave-assisted extraction

✉ Doan Pham Minh
phamminhdoan@duytan.edu.vn;
doan.phamminh@mines-albi.fr

[1] Institute of Chemical Technology, Vietnam Academy of Science and Technology, 1 Mac Dinh Chi Str., Dist. 1, Ho Chi Minh City, Vietnam

[2] Graduate University of Science and Technology, Vietnam Academy of Science and Technology, 18 Hoang Quoc Viet Street, Cau Giay District, Hanoi, Vietnam

[3] Coastal Plains Soil, Water and Plant Research Center, USDA-ARS, 2611 West Lucas Street, Florence, SC 29501, USA

[4] Advanced Energy Research and Technology and Materials Science and Chemical Engineering Department, Institute of Gas Innovation and Technology, Stony Brook University, Stony Brook, NY 11794-2275, USA

[5] Faculty of Engineering, School of Chemical and Energy Engineering, Universiti Teknologi Malaysia (UTM), 81310 Johor Bahru, Johor, Malaysia

[6] Institute for Materials Chemistry and Engineering, Kyushu University, 6-1, Kasuga Koen, Kasuga 816-8580, Japan

[7] Transdisciplinary Research and Education Center of Green Technology, Kyushu University, Kasuga 816-8580, Japan

[8] Institute of Research and Development, Duy Tan University, Da Nang 550000, Vietnam

[9] Université de Toulouse, IMT Mines Albi, UMR CNRS 5302, Centre RAPSODEE, Campus Jarlard, 81013 Albi cedex 09, France

[10] Center of Excellence for Green Energy and Environmental Nanomaterials (CE@GrEEN), Nguyen Tat Thanh University, 300A Nguyen Tat Thanh, District 4, Ho Chi Minh City 755414, Vietnam

MPO	Methane partial oxidation
MWCNT	Multi-walled carbon nanotubes
MWH	Microwave heating
M/GR	MWCNT/layered graphene composite
M/CSCNT	MWCNT/cup-stacked CNT composite
OMR	Oxy-CO_2 methane reforming
PSA	Pressure swing adsorption
PTO	Lead titanate
PZT	Ferroelectric lead zirconate titanate
SEM	Scanning electron microscopy
SMR	Steam methane reforming
TEM	Transmission electron microscopy
VHSV	Volume hourly space velocity
WGSR	Water–gas-shift reaction

Introduction

Global energy consumption steadily increased from 8.8 billion tonnes oil equivalent (btoe) in 1990 to 13.865 btoe in 2018 (BP Statistical Review of World Energy). Despite the progress made in the development of alternative sources over the past decades, fossil fuels including coal, oil and natural gas still account for approximately 84.7% of the total global energy consumption in 2019 (BP Statistical Review of World Energy). Among fossil fuels, natural gas burns the cleanest and as such, is considered the bridge fuel to renewables (Védrine 2005). Natural gas can be directly used to heat buildings and used as a feedstock to produce fuels and chemicals (Védrine 2005). For natural gas conversion, the most common route is via conversion to synthesis gas or syngas, which is a mixture of varying amount of hydrogen, carbon monoxide, and carbon dioxide. Syngas is an important platform for chemical gas mixture because it is commercially used for the production of ammonia, methanol, mixed alcohols, oxygenates, and hydrocarbons via Fischer–Tropsch synthesis (Liu et al. 2009). According to Higman (2017), total syngas usage increased 11% from 120.9 million Nm^3/h in 2016 to 134.3 million Nm^3/h in 2017 for all end-use products. Two major syngas production processes are gasification using coal, gas, petcoke, petroleum, biomass and waste as primary feedstocks (Raje and Davis 1997) and methane reforming. In 2017, gasification accounted for about 42% or 173 GWh, and methane reforming accounted for the remaining 58% or 240 GWh power generation (Higman 2017). At the industrial scale, methane reforming includes steam methane reforming (SMR, Eq. 1) and methane partial oxidation (MPO, Eq. 2). Steam methane reforming is still the dominant process in the syngas production industry. Overall, there are several major disadvantages of steam methane reforming (Tsang et al. 1995). It needs excessive superheated steam for the process at high temperature, causing high operating cost. Also, steam methane reforming is a highly endothermic reaction and the process requires temperature typically above 800–900 °C, which can hasten catalyst deactivation. The energy to meet the endothermicity requirement is usually supplied from the combustion of a fuel resulting in a large CO_2 emission. The methane partial oxidation reaction occurs at a typical high temperature around 1400 K. The operating temperature can be greatly reduced as low as 1023 K for high yields of syngas production with the use of a catalyst (York et al. 2003). However, there are several drawbacks related to methane partial oxidation that limits its application (York et al. 2003) (Tsang et al. 1995; York et al. 2003). First, hot-spot may occur in the catalyst bed which causes safety and efficiency reductions issues. Second, the purification of product syngas related to O_2 removal is expensive. Finally, coke formation on catalyst surface needs to be addressed.

Steam methane reforming:

$$CH_4 + H_2O \rightleftharpoons CO + 3H_2 \qquad \Delta H_{298\,K} = +206\ \text{kJ/mol} \tag{1}$$

Methane partial oxidation:

$$CH_4 + {}^1\!/_2O_2 \rightleftharpoons CO + 2H_2 \qquad \Delta H_{298\,K} = -36\ \text{kJ/mol} \tag{2}$$

Dry reforming of methane:

$$CH_4 + CO_2 \rightleftharpoons 2CO + 2H_2 \qquad \Delta H_{298\,K} = +274\ \text{kJ/mol} \tag{3}$$

Of particular interest is methane oxidation using a well-known greenhouse gas, CO_2, known as dry reforming of methane (Eq. 3). Both reactants of the dry reforming of methane reactions are the main compounds of natural gas and biogas which is considered as an important renewable resource (Jain et al. 2019). The dry reforming of methane reaction also needs a catalyst to control the kinetic and the selectivity of the reaction. Nickel-based catalysts are the most used for the dry reforming of methane reaction (Alia et al. 2020; Meloni et al. 2020). However, the major issue is catalyst deactivation by coke and carbon formation on catalysts' surface and by thermal sintering (Fischer and Tropsch 1928; Chen et al. 2012). In fact, according to Eq. 3, the dry reforming of methane reaction is highly endothermal and requires high reaction temperature (above 700 °C), which can speed up both catalyst thermal sintering and local "cold-spot" inside catalyst beds (Chen et al. 2012). So, heat transfer control also plays important role in dry reforming of methane. This latter can be achieved by using microwave-assisted technology.

Microwave-assisted chemical processes using commercial microwave ovens were reported by Giguere et al. (1986).

Since then, this technique has shown promise as an alternative technique in extraction (Eskilsson and Björklund 2000; Mandal et al. 2007), environmental engineering (Jones et al. 2002a, b), synthesis (Nüchter et al. 2004), pyrolysis (Motasemi and Afzal; 2013) and reforming (Fidalgo et al. 2008). Compared to conventional heating, the microwave heating offers several advantages including: higher heating rate, better heating control, reduction of equipment size, time and energy savings, etc. (Jones et al. 2002a, b; Motasemi and Afzal 2013).

To date, the dry reforming of methane reaction performed with a conventional heating system has actively studied during the last decades, as illustrated by several recent reviews in the literature (Abdulrasheed et al. 2019; Aramouni et al. 2018; Arora and Prasad 2016; Jang et al. 2019; Lavoie 2014; Muraza and Galadima 2015). Some of these studies evoked microwave-assisted technology as a novel approach for the dry reforming of methane reaction (Shah and Gardner 2014). However, microwave-assisted dry reforming of methane (DRM) was only recently reviewed by Nguyen et al. (2020), and this latter did not cover all the aspects of microwave-assisted DRM such as the thermodynamics of the process, the influence of operating conditions, the energy consumption versus conventional heating. So, the objective of this paper is to address a comprehensive synthesis of research work dedicated to microwave-assisted DRM with focus on challenges and opportunities of this process.

Thermodynamics of dry reforming of methane

Dry reforming of methane reaction produces CO and H_2 as the main products from CH_4 and CO_2. CH_4 and CO_2 are chemically stable because of their high bonding energy. Their transformation needs severe temperature conditions to activate them. Thus, thermodynamic study on the equilibria of the dry reforming of methane reaction is useful to determinate the thermodynamic limit of the process. In the literature, work has been done on the thermodynamic equilibrium of this process (Chein et al. 2015; Li et al. 2008; Nematollahi et al. 2012; Nikoo and Amin 2011; Pashchenko 2017; Pham Minh et al. 2018; Protasov et al. 2012). The common feature of these studies relates to the basis of Gibbs free energy minimization method. The principle of this method has been detailed in previous studies (Li et al. 2008; Nematollahi et al. 2012; Nikoo and Amin 2011; Protasov et al. 2012). Different parameters of the dry reforming of methane have been investigated in particular: (1) the influence of the temperature and pressure on the conversion of CH_4 and CO_2 and the selectivity in CO and H_2; (2) the influence of the composition of the initial mixture of CH_4 and CO_2; and (3) the formation of by-products like C_s and water, and also light hydrocarbons.

The dry reforming of methane reaction generates CO and H_2 as the main gaseous products, but other by-products such as solid carbon (C_s), water and light hydrocarbons are also formed. Among them, light hydrocarbons are formed at the very low quantity (Nikoo and Amin 2011). In addition to the main dry reforming of methane reaction (Eq. 3), the following reactions can also take place:

Boudouard reaction:

$$2CO \rightleftharpoons C_s + CO_2 \qquad \Delta H_{298\,K} = -172 \text{ kJ/mol} \tag{4}$$

Methane cracking :

$$CH_4 \rightleftharpoons C_s + 2H_2 \qquad \Delta H_{298\,K} = +75 \text{ kJ/mol} \tag{5}$$

Water - gas - shift:

$$CO + H_2O \rightarrow CO_2 + H_2 \qquad \Delta H_{298\,K} = -41 \text{ kJ/mol} \tag{6}$$

Steam reforming of carbon:

$$C_s + H_2O \rightarrow CO + H_2 \qquad \Delta H_{298\,K} = +131 \text{ kJ/mol} \tag{7}$$

Using FactSage software, which bases also on the Gibbs free energy minimization method (Pham Minh et al. 2018), the thermodynamic equilibrium of different CH_4 and CO_2 mixtures under different physicochemical conditions could be obtained as presented below. According to Pham Minh et al. (2020), Fig. 1 shows the results obtained for an equimolar mixture of CH_4 and CO_2 at 1 bar. Below 550 °C, solid carbon (C_s) and H_2O are predominant species, together with CH_4 and CO_2. By increasing the temperature, all these species are converted to form syngas. At 900 °C, the conversion of CH_4 and CO_2 can reach 98.1 and 97.3%, respectively. Solid carbon can be practically negligible at this temperature from thermodynamic point of view.

From the stoichiometry of Eq. 3, it is evident that the dry reforming of methane reaction is favourable at low pressure. However, when the dry reforming of methane reaction is integrated into a multi-step process, the realization of this reaction at high pressure is sometimes necessary to optimize global energy balance. This is the case for the production of green hydrogen from landfill gas using steam reforming followed by the water–gas-shift reaction (WGSR) and pressure swing adsorption (PSA) steps (Grouset and Ridart 2018). Figure 2 shows the influence of the pressure on thermodynamic equilibrium of a mixture containing initially 1 mol of CH_4 and 1 mol of CO_2 at 800 and 900 °C. Increasing the pressure from 1 to 30 bar strongly decreases the equilibrium amount of both H_2 and CO at 800 and 900 °C, which illustrates the negative impact of the pressure on this process (Fig. 2a, b). At 900 °C, the conversion of CH_4 and CO_2 decreases from 98.1 and 97.3% at 1 bar to 76.0 and 71.3% at 30 bar (Fig. 2c). In parallel, the equilibrium amount of solid

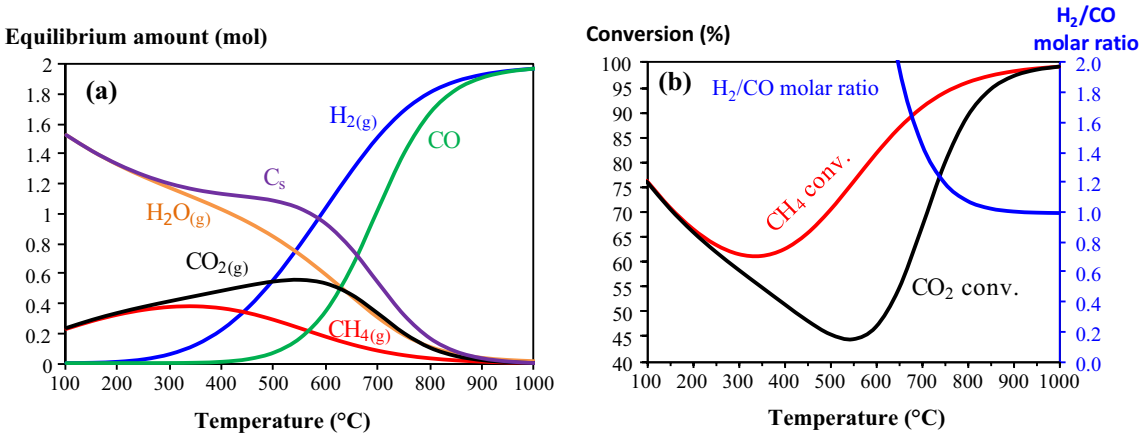

Fig. 1 Thermodynamic equilibrium of a mixture containing initially 1 mol of CH_4 and 1 mol of CO_2 at 1 bar (**a**); conversion of CH_4 and CO_2 and molar ratio of H_2/CO. The transformation of CH_4 and CO_2 into H_2 and CO is only favoured at high temperature, e.g. above 800 °C. The molar ratio of H_2/CO could theoretically reach 1 at high temperature. Reprinted by permission from Springer Nature (Pham Minh et al. 2020), Copyright 2020

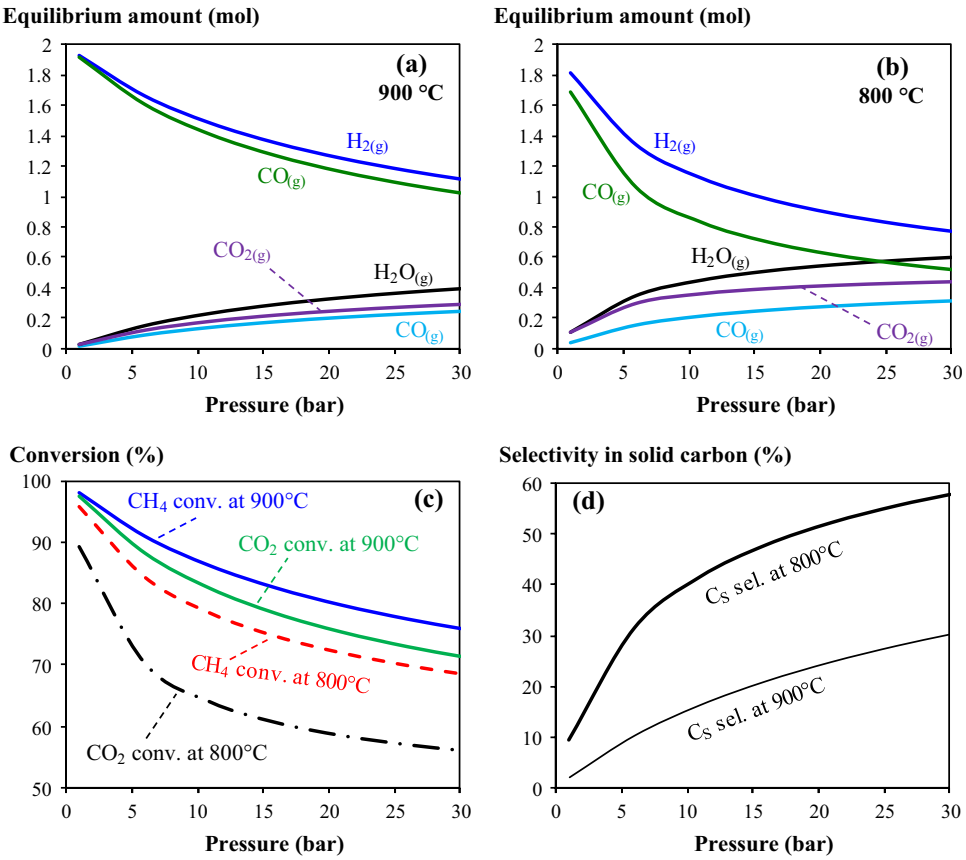

Fig. 2 Effect of the pressure on the thermodynamic equilibrium of a mixture containing initially 1 mol of CH_4 and 1 mol of CO_2 at 800 and 900 °C. At high temperature of 800 and 900 °C, the increase in the total pressure highly decreases the transformation of CH_4 and CO_2 into syngas and highly favours the formation of solid carbon

carbon quickly increases with the increase in the pressure (Fig. 2d). The selection of operating pressure for the dry reforming of methane at a large scale must be carefully examined taking into account other factors of the global process. It is worth noting that the steam reforming of methane is usually performed at around 900 °C and 15–30 bar with a molar ratio of steam/methane close to 3/1 (Grouset and Ridart 2018).

In the dry reforming of methane reaction, the formation of solid carbon (C_s) highly impacts the stability of catalyst. This can be limited by adjusting the content of CO_2 in the initial mixture of CH_4 and CO_2. Figure 3 shows the influence

of the molar ratio of CH_4/CO_2 at two different pressures of 1 and 15 bar.

As expected, under a given pressure, increasing the content of CO_2 is favourable for CH_4 conversion (Fig. 3a). At 1 bar and 700 °C, CH_4 conversion can reach 97% at $CH_4/CO_2 = 1/3$. To get this CH_4 conversion at $CH_4/CO_2 = 1/2$ and 1 bar, the temperature must be equal to 750 °C. Once again, increasing the pressure does not favour the methane conversion. At 15 bar and 900 °C, which are the typical conditions used in steam reforming of methane, CH_4 conversion can reach 92 and 97% at $CH_4/CO_2 = 1/2$ and 1/3, respectively.

Figure 3b shows CO_2 conversion, but this is not really representative of real situations since CO_2 is in large excess. Figure 3c, d presents the selectivity in H_2 and CO. The negative influence of increasing the pressure can be clearly observed. In addition, CH_4/CO_2 ratio strongly influences the formation of H_2 and CO via the reserve water–gas shift (Eq. 6). Under a given experimental condition of pressure and CH_4/CO_2 ratio, and by increasing the temperature, there is a maximum in the formation of H_2. In fact, H_2 formation from the dry reforming of methane reaction is favourable by increasing the reaction temperature. Then, this H_2 is consumed in Eq. 6 by reacting with CO_2 which is in large excess

Figure 3e, f presents the formation of H_2O and C_s as the two major undesirable by-products of the dry reforming of methane reaction. Within the temperature and pressure ranges simulated in this study, and regardless the CH_4/CO_2 ratio = 1/2 or 1/3, water formation is inevitable because of the omnipresence of the reserve water–gas shift (Eq. 6). As previously observed for H_2 formation, under a given experimental condition of pressure and CH_4/CO_2 ratio, increasing the temperature leads to a minimum of H_2O formation, i.e. close to 800 °C for the molar ratio of CH_4/CO_2 of 1/2 and at 1 bar. The coke formation can be theoretically avoided by increasing the reaction temperature, since the steam reforming of carbon (Eq. 7) is highly endothermal. As an example, at 1 bar and with the molar ratio of CH_4/CO_2 equal to 1/3, C_s selectivity can be completely avoided above 700 °C

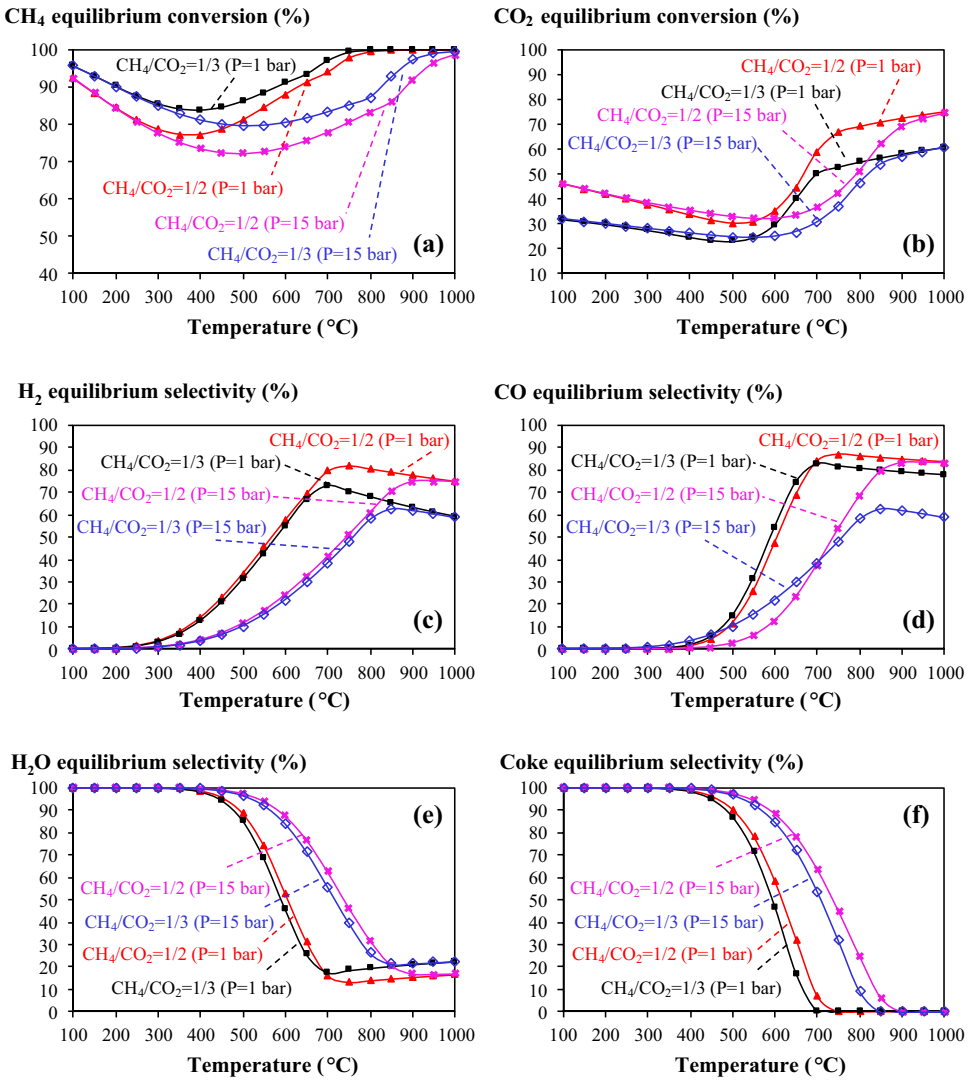

Fig. 3 Influence of the molar ratio of CH_4/CO_2 on the dry reforming of methane reaction at 1 and 15 bar. At a given temperature and total pressure, the decrease of the molar ratio of CH_4/CO_2 allows increasing CH_4 conversion and decreasing coke formation

In all cases, the formation of light hydrocarbons (C2 to C4) is possible but only at traces amounts as previously observed (Nikoo and Amin 2011).

As a partial conclusion, the reaction of CH_4 with CO_2 is complex with the presence of different chemical equilibria. In general, the dry reforming of methane reaction is favourable at high temperature, low pressure, and the low molar ratio of CH_4/CO_2. However, when working with low CH_4/CO_2 ratio, the temperature must be carefully selected to avoid the detrimental effect on the formation of H_2.

Microwave heating technology

Principles of microwave heating

Microwaves are electromagnetic radiations whose wavelength range is from 1 to 1 mm corresponding to a frequency range of 0.3–300 GHz. Generally, microwave heating (MWH) is conducted at 0.9 or 2.45 GHz to avoid or minimize any possible interference with the communication applications (Meredith 1998). Unlike conventional heating that is basically relied on the heat transfer of hot medium, microwave heating is created through the interactions of the objects with the electric and magnetic fields. Thus, microwave heating offers several advantages comparing to conventional one, including (1) non-contacting, quick and selectable heating; (2) rapid starting and stopping of the heating; and (3) more safety and easier automation (Jones et al. 2002a, b; Menéndez et al. 2010; Zhang and Hayward 2006). Consequently, applying microwaves causes reducing in the equipment size and processing time. Therefore, microwave heating is now not only applied for industrial wood drying, food processing, and rubber vulcanization, but also studied in various areas, such as, ceramic and polymer processing (Komarneni et al. 1992; Hoogenboom and Schubert 2007; Wiesbrock et al. 2004), environmental applications (Jones et al. 2002a, b; Verma and Samanta 2018; Zhang and Hayward 2006; Zlotorzynski 1995), biofuels and chemical productions (Aravind et al. 2020; Hassan et al. 2020), and metallurgy and mineral processing (Jones et al. 2002a, b; Kingman et al. 2004). Particularly, there is an increasing interest in the study of heterogeneous gas-phase catalysis under microwave heating (Zhang and Hayward 2006; Durka et al. 2009), such as NH_3 decomposition (Guler et al. 2017), CH_4 decomposition (Domínguez et al. 2007a, b; Zhang et al. 2003), H_2S decomposition (Xu et al. 2017a, b), NO_x and SO_2 reduction (Peng et al. 2017; Zhang et al. 2001), CO_2 reforming of CH_4 (Fidalgo and Menéndez 2013; Lim and Chun 2017; Zhang et al. 2003) and recently steam reforming of alcohols (Durka et al. 2011; Gündüz and Dogu 2015; Sarıyer et al. 2019). It was found that microwave heating apparently induces higher reactants conversions and product yields compared to conventional heating at the same operating temperature due to the formation of hot spots (Fidalgo et al. 2008, 2010; Fidalgo and Menéndez 2012; Zhang et al. 2003).

Practically, both components of the high-frequency electromagnetic radiation are responsible for microwave heating. However, dielectric heating caused by the electric field component is often used to represent microwave heating, whereas the heating effect induced by the magnetic one is seldom mentioned due to insufficient knowledge (Sun et al. 2016). Dielectric heating occurs when the dipoles collide with each other while trying to align themselves with the high-frequency electric field by rotation. Accordingly, the heating ability of a dielectric is described by its dielectric loss tangent ($\tan\delta$) as given in Eq. 8:

$$\tan\delta_{\varepsilon} = \varepsilon''/\varepsilon' \tag{8}$$

The real (ε') and imaginary (ε'') parts of permittivity represent the abilities to propagate microwaves into the object and to generate heat by dissipation of microwave power, respectively (Jones et al. 2002a, b; Menéndez et al. 2010). It is widely accepted that a good microwave absorber must have loss tangent value greater than 0.1 (Beneroso and Fidalgo 2016; Metaxas and Meredith 1983; Rossi et al. 2017). Dielectric properties of a specific sample rely upon its anisotropy, homogeneity, surface roughness, and the applied temperature and frequency (Janezic et al. 2001). Ignoring the effect of factors related to its nature and the applied frequency, the loss tangent of a sample generally increases with its temperature at a frequency of 900 MHz or 2.45 GHz (Gabriel et al. 1998; Janezic et al. 2001; Westphal and Sils 1972; Zhang et al. 2002). Many solid materials, such as alumina and silica (Nightingale 2001; Westphal and Sils 1972) which are commonly used as effective catalyst supports, are classified as very low-lossy material at room temperature. However, their heating ability rises rapidly when the temperature is above certain point as can be seen in Table 1. Besides, some moderate lossy materials, such as carbon-coated on SiO_2 (C-SiO_2) and platinum-coated on carbon (Pt/C), exhibit a double increase in their dielectric loss tangent at over 800 °C compared to that at room temperature. Practically, these materials could be employed in microwave-assisted DRM application due to its high operating temperature which favours the ability to absorb microwave (Zhang et al. 2018a, b, c). Thus, understanding the dielectric properties of a catalytic/supporting material in its expected operating temperature range is essential. Unfortunately, the available studies usually focused on the dielectric properties of the materials in the wide frequency range without considering the response to temperature since their target application is for microwave absorption, not for heating (Benedito et al. 2012; Bhattacharya and Basak 2016;

Table 1 Dielectric loss tangent (tan δ_ε) of common substances

Material	Temperature (°C)	Frequency (GHz)	Dielectric properties			References
			ε'	ε''	$\tan\delta_\varepsilon$	
Microwave transparent						
Vacuum	25	2.54	1.00	0	0	Durka et al. (2009)
Air	25	2.54	1.0006	0	0	Durka et al. (2009)
n-hexane	20	2.54			0.02	Zhu and Chen (2014)
Styrofoam	25	3	1.03	0.0001	0.0001	Durka et al. (2009)
PTFE	25	10	2.08	0.0008	0.0004	Durka et al. (2009)
Titanium oxide	25	2.54	50	0.25	0.005	Durka et al. (2009)
Magnesium oxide	25	2.54	9	0.0045	0.0005	Durka et al. (2009)
Glass (pyrex)	25	3	4.82	0.026	0.0054	Durka et al. (2009)
Fused silica	25	5.5			< 0.0003	Durka et al. (2009)
	1165				0.01	
Fused quartz	25	2.54	3.78	< 0.001	0.00025	Gupta and Leong (2008)
Silicon	25	1	4.3	< 0.05	< 0.0116	Meredith (1998)
Alumina (dynallox 100)	590	2.54	10.37	0.027	0.0026	Bhattacharya and Basak (2016)
	980		11.06	0.15	0.01356	
	1340		11.64	0.74	0.06412	
Glass–ceramics (Li_2O–Al_2O_3–SiO_2)	20	9.37			0.011	McMillan and Partridge (1972)
	400				0.021	
Microwave absorber						
Water	20	2.54	77.4	9.48	0.122	Gabriel et al. (1998)
Methanol	20	0.9	32.1	8.49	0.265	
	20	2.54	21.9	14.6	0.665	
Ethanol	20	2.54	24.3	22.86	0.941	
Hexanol	20	0.9	3.96	2.25	0.568	
	20	2.54	3.43	1.17	0.341	
Glycerol	20	0.9	8.41	6.39	0.759	
	20	2.54	6.33	3.42	0.540	
Nitrobenzene	20	0.9	33.7	7.73	0.229	
	20	2.54	25.2	14.7	0.584	
Zirconium oxide	25	2.54	20	2	0.1	Durka et al. (2009)
Zinc oxide	25	2.54	3	3	1	Durka et al. (2009)
Silicon carbide	25	3			0.58	Westphal and Sils (1972)
	20	2.45	30	11	0.3667	Meredith (1998)
C–SiO_2	25	2.54	13.7	6	0.437	Hamzehlouia et al. (2018)
	> 800	2.54	< 15	12	> 0.8	
Pt/C	20	2.54			< 0.27	Gangurde et al. (2017)
	850	2.54			< 0.4	

Horikoshi et al. 2012; Wang et al. 2019; Xiong et al. 2017; Zhang et al. 1999).

In the case of conductor materials, an electric current will be created under the effect of the high-frequency electric field, causing heating due to the collisions of the charged particles with their neighbouring atoms and molecules (Meredith 1998). These losses dominate in conductors, whereas the dielectric losses dominate in lossy dielectrics such as water, polar solvent, glass, and ceramic. However, in some cases such as microwave heating of electrolyte solutions (Horikoshi et al. 2012) or carbonaceous materials (Menéndez et al. 2010), both mechanisms are involved to heat the objects in the high-frequency electric field, resulting in an enhancement of heating rate.

To date, the microwave magnetic heating has been rarely ascribed although its superior advantages over the electric heating for several ferrites and powder conductive materials such as Fe_3O_4, WC, Fe, and Co were experimentally proved by Cheng et al. (2001, 2002). A microwave-assisted synthesis method was then demonstrated to prepare some

ferrites that have new crystal structure such as $ZnFe_2O_4$, $NiFe_2O_4$, $BaFe_{12}O_{19}$, $CoFe_2O_4$, and Fe_3O_4 from stoichiometric mixtures of constituent oxides (Roy et al. 2002). The authors observed that the major changes in the structural phase of the produced ferrites and their magnetic properties are mainly caused by the magnetic field component. The crystallization of ferroelectric lead zirconate titanate (PZT) (Bhaskar et al. 2007) and lead titanate (PTO) (Zhang et al. 2018a, b, c) on substrates was reported to be able to occur at only 450 °C in the predominant magnetic field region of a single-mode microwave applicator, whereas SiC rods need to be employed as a microwave susceptor if the crystallization of ferroelectric lead zirconate titanate is performed in a multi-mode one where the predominant magnetic field regions cannot be determined (Antunes et al. 2018). At this moment, there are enough studies to conclude that the magnetic losses contribute significantly to the microwave heating of not only magnetic materials but also conductors, semiconductors and other composite materials (Bhattacharya and Basak 2016; Cao et al. 2010; Haneishi et al. 2017; Rosa et al. 2016; Wen et al. 2011; Zhang et al. 1999); thus, it deserves to receive more attention.

Similar to the dielectric heating, the magnetic heating ability of a material is described by its magnetic loss tangent ($\tan\delta_\mu$) as given by Eq. 9:

$$\tan\delta_\mu = \mu''/\mu' \tag{9}$$

The real (μ') and imaginary (μ'') parts of permeability represent the amount of energy stored and lost, respectively (Durka et al. 2009; Sun et al. 2016). Table 2 shows that a ferrite could not be considered as a good microwave absorber with respect to only its dielectric loss tangent. However, with respect to both values, all of them are suited for microwave heating applications.

In addition to the above-mentioned factors, the heating efficiency is also affected by the penetration depth in which the microwave power decreases to 37% of its value at the object's surface (Durka et al. 2009; Sun et al. 2016). The penetration depth apparently decreases with increasing frequency, dielectric and magnetic losses. In the heating applications where the frequencies of 900 MHz and 2.45 GHz are commonly used, a material that has a high heating ability exhibits a low penetration depth whereas low-lossy materials such as high purity quartz, Teflon, and other plastic can be almost transparent to microwaves (Barbosa-Canovas and Ibarz 2014; Menéndez et al. 2010). Both experimental (Cao et al. 2010; Yoshikawa et al. 2006) and theoretical (Hotta et al. 2011) studies revealed that bulk metals totally reflect microwaves and can only undergo surface heating, due to the so-called skin effect. Meanwhile, powdered metals can be considered as good microwave absorbers if their particles are fine enough compared to their penetration depths in order to be effectively heated in the electromagnetic fields. Table 3 shows the estimated penetration depth of common bulk metals. Detailed calculation method for estimating the penetration depth can be found in literatures (Atwater and Wheeler 2004; Gupta and Leong 2008).

Microwave susceptors

It has been known that low-lossy or transparent materials could not be rapidly heated to elevated temperatures which are required to conduct the dry reforming of methane reaction efficiently. All reactants and most common catalysts used in the dry reforming of methane reaction such as Ni-based catalysts supported on SiO_2, Al_2O_3 or other mesoporous materials (Wang et al. 2018; Abdullah et al. 2017; Lovell et al. 2015) showed relatively low microwave absorption due to their low dielectric loss tangent (Fidalgo et al. 2011). A long warm-up time

Table 2 Dielectric and magnetic properties of some ferrites at 25 °C and 2.45 GHz (Bhattacharya and Basak 2016)

Material	Dielectric properties			Magnetic properties		
	ε'	ε''	$\tan\delta_\varepsilon$	μ'	μ''	$\tan\delta_\mu$
Fe_3O_4	12.51	0.25	0.02	1.51	0.3	0.199
$BaFe_{12}O_{19}$	1.465	0.052	0.036	1.105	0.071	0.064
$CuFe_2O_4$	1.507	0.091	0.06	1.029	0.106	0.103
$CuZnFe_4O_4$	1.595	0.089	0.056	1.038	0.209	0.201
$NiZnFe_4O_4$	1.313	0.123	0.094	1.080	0.201	0.186

Table 3 Calculated penetration depth of some metals 25 °C and 2.45 GHz (Atwater and Wheeler 2004; Bhattacharya and Basak 2016; Stefanidis et al. 2014)

Metals	Mg	Al	Zn	Au	Cu	Ag	Fe	Zr	Ni	Co
Penetration depth (μm)	2.2	1.7	2.5	1.5	1.3	1.3	3.2	6.7	2.7	2.5

is necessary for the transparent materials to be heated to the desired temperature when they start absorbing microwaves. In some cases, these materials even could not be heated to such point without using a microwave susceptor which must be a highly lossy material (Fidalgo et al. 2011; Horikoshi et al. 2018). There are two ways to overcome this critical issue: (1) enhancing the microwave absorbing ability of the material by doping with or coating on other microwave absorbers or susceptors; and (2) using the external microwave susceptors to heat the material by thermal radiation (Bhattacharya and Basak 2016). Both techniques have their own advantages and drawbacks so choosing one depends on what would be expected. The former invasive route alters the physicochemical properties of the original material, but it is more effective in assisting them to be directly heated by microwaves. On the contrary, simply incorporating with the susceptors does not affect the material but heating by thermal radiation is obviously less effective comparing to direct heating by microwave radiation. However, as the material becomes more lossy to be able to absorb microwaves at a higher temperature, it then undergoes a two-way heating: conventional heating from the surface by susceptor-generated thermal radiation and microwave heating from the centre, resulting in a more uniform heating.

Carbon-based susceptor

Except for coal, carbonaceous materials such as graphite, activated carbon, carbon nanotube, and bio-char have already been demonstrated to be effective susceptor for many microwave heating applications because of their high conductivity and dielectric loss tangent as can be seen in Table 4. It is well known that a larger amount of delocalized π-electrons presented in the carbonaceous materials results in a larger microwave absorbing ability (Beneroso and Fidalgo 2016). Therefore, low-lossy coal has been reported to become a highly lossy material at the end of the carbonization process (Peng et al. 2012).

Actually, carbonaceous materials could be used as the active catalysts for the dry reforming of methane reaction (Li et al. 2019). However, as indicated in the following section, they are definitely consumed by CO_2 gasification that takes place during the reforming process (Fidalgo and Menéndez 2013). That's why they are rarely employed as external susceptors for microwave-assisted DRM, while they are commonly used in other microwave heating applications (Antunes et al. 2018; Horikoshi et al. 2018). Li et al. (2017) reported an unstable activity of a heterogeneous mixture of Ni-based catalyst and bio-char on the dry reforming of methane reaction which is mainly caused by CO_2 gasification reaction. It was observed that the production of syngas and its composition decreased significantly with time on stream during only 120 min of operation. Recently, Hamzehlouia et al. (2018) develop a novel C-SiO_2 microwave susceptor which has excellent loss tangent comparing to the conventional receptor particle. Carbon was coated by SiO_2 resulting in no reverse impact on the performance of Ni/Al_2O_3 catalyst; however, this approach is quite complicated. Therefore, carbonaceous materials have been preferably investigated as either catalyst supports or active catalysts, and related studies were reviewed in the next section.

Table 4 Dielectric properties of carbon-based materials at 25 °C and 2.45 GHz

Carbon material	Dielectric constant (ε')	Loss factor (ε'')	Loss tangent ($\tan \delta_\varepsilon$)	References
Long-flame coal	3.06	0.02	0.006	Liu et al. (2018)
Brown coal	7.41	0.10	0.013	Liu et al. (2018)
Bituminous coal	3.48	0.13	0.037	Peng et al. (2012)
Carbonized bituminous coal[a]	120	88	0.733	Peng et al. (2012)
Bio-char[b]	2.82	0.24	0.085	Salema et al. (2013)
Pyrolysis bio-char[c]	6.00	1.22	0.203	Ellison et al. (2017)
Carbon black	9.29	1.75	0.188	Hotta et al. (2011)
Activated carbon	1.94	1.76	0.907	Yin et al. (2018)
Graphite[d]	17.61	5.01	0.28	Hotta et al. (2011)
CNTs-HPCFs	13.4	5.11	0.381	Qiu and Qiu (2015)

CNTs-HPCFs Carbon nanotubes-hollow porous carbon fibres

[a]Dielectric properties of bituminous coal was determined during pyrolysis in which the sample was step-heated to 750 °C with ramp rate of 5 °C/min

[b]Bio-char is made of oil palm shell

[c]Pyrolysis char is made of live oak

[d]Pure carbon

Non-carbon based susceptor

Although the non-carbon-based susceptors usually showed lower heating efficiencies comparing to the carbonaceous ones (Benedito et al. 2012; Bhattacharya and Basak 2016), they have been preferably used in the microwave-assisted DRM applications because of unavoidable activity of the carbon-based susceptor on the dry reforming of methane reaction (Fidalgo and Menéndez 2013). In addition to the most common used non-carbon-based susceptors in microwave heating applications such as SiC and CuO, some metals, which have good microwave absorbing ability at small particle size, and ferrites have been recently introduced as potential susceptors for various microwave heating applications (Bhattacharya and Basak 2016). However, only SiC has been employed as catalyst supports (Bhattacharya and Basak 2016). However, only SiC has been employed as catalyst supports (Zhang et al. 2018a, b) to enhance the coupling effect between the microwaves and catalysts used in the dry reforming of methane reaction. SiC is an inert material, thus does not interfere with any reactions, and consequently, a stable performance of SiC supported catalyst on microwave-assisted DRM was observed during 50 h of reaction (Zhang et al. 2018b). Since commercially available silicon carbide has a low specific surface area, it cannot be employed as an effective support for any catalyst. Zhang et al. (2018a) synthesized SiC-based supports composed of $SiC{\cdot}SiO_2$ and $Al_2O_3{\cdot}SiC$ ceramic foams. Although Al_2O_3 has been shown to be superior to SiO_2 as support of nickel catalyst for the conventional dry reforming of methane with respect to both activity and stability (Xu et al. 2019), the catalytic activity of $Fe/(SiC{\cdot}SiO_2)$ in microwave-assisted DRM was reported to be higher than that of $Fe/(Al_2O_3{\cdot}SiC)$ due to its greater microwave absorbing capability.

While supported nickel-based catalysts have been widely investigated for the dry reforming of methane (Wang et al. 2018), using Ni supported on SiC catalyst for microwave-assisted DRM has not been demonstrated. Hawangchu et al. (2010) observed that Ni/SiC bed reached a much lower temperature compared to the bare SiC after being heated for 5 min in the microwave at the same power level. This observation was simply explained by consideration of the microwave reflection behaviour of Ni metal particles. In fact, metallic magnetic Ni-based material can behave either as a microwave reflector or absorber depending on its particle size and penetration depth at certain working conditions such as temperature and frequency (Bhattacharya and Basak 2016). Due to its high magnetic loss tangent, coating nickel on the surface of a high lossy dielectric material may enhance its microwave absorption capability (Zhao et al. 2015). Therefore, Ni supported on SiC with a proper layer thickness would be a promising catalyst for microwave-assisted DRM. Another approach that should be tried is mixing the supported Ni-based catalysts with SiC. Chen et al. reported that simply covering each thin layer of low-lossy sawdust with a thin layer of SiC microwave absorber can deliver uniform heating for pyrolysis of sawdust samples (Chen et al. 2008).

In addition, there are many promising approaches that were successfully demonstrated in other microwave heating applications that have not been investigated for microwave-assisted DRM yet. The perovskite-type mixed oxide, such as $BaMn_{0.2}Cu_{0.8}O_3$ was proved to be an effective external susceptor for improving the activity of NiS/Al_2O_3 and CoS/Al_2O_3 catalyst in microwave-assisted decomposition of H_2S (Xu et al. 2017b). Zhang et al. (1999) observed that the loss tangent of γ-Al_2O_3 increased significantly by either coating or mixing it with MoS_2, which is a good microwave absorber, leading to an enhanced activity for the decomposition of H_2S under microwave radiation. Based on these results, Xu et al. (2017a) prepared a mechanical mixture of CoS, MoS_2, and γ-Al_2O_3 which work as a catalyst, as a catalyst and microwave susceptor and as a porous support, respectively. Consequently, the outstanding catalytic activity of $CoS\text{-}MoS_2/\gamma\text{-}Al_2O_3$ for decomposition of H_2S under microwave radiation has been attributed to the synergistic effects of all components. Similarly, these approaches could be employed in the microwave-assisted DRM. For example, Ni-WC_x was proposed as an active bi-functional catalyst for the conventional dry reforming of methane (Zhang et al. 2015), whereas WC was reported as a good microwave absorber (Cheng et al. 2001 2002). Thus, Ni-WC_x catalyst may exhibit enhanced activity in microwave-assisted DRM. Besides, perovsikites and ferrites are deserved to be investigated as both catalysts and susceptors in microwave-assisted DRM due to their excellent microwave absorbing ability as well as catalytic activity (Benrabaa et al. 2013; Caprariis et al. 2015; Sheshko et al. 2017).

Microwave heating apparatus

Basically, a microwave heating system consist of four parts: (1) power source, (2) microwave generator, (3) applicator or cavity in which the target material is put, and (4) waveguide for transporting microwaves generated to inside the cavity (Haque 1999). However, the main differences between the studied microwave-assisted catalytic systems arise from the temperature controlling method and the design of the microwave cavity. The power output of magnetron could be controlled by either simply on–off mode (Li et al. 2011) or by varying the electrical power input to the high-voltage transformer unit (Fidalgo et al. 2008). In the former case, the desired average power will be obtained by periodically turning on/off the power supply with full load. Meanwhile, in the latter case, the more precise power output can be controlled by altering the

voltage or current amplitude. In order to control reaction temperature precisely, there is also a need for choosing the correct temperature measurement solution, which is not a straightforward task. An inconel-sheathed thermocouple was reported to be able to continuously record inside temperature without electrical noise and arcing by earthing the sheathed thermocouple through the microwave oven casing (Hogan and Mori 1990). However, this thermocouple was only used to measure up to the boiling point of water; thus, employing such thermocouples under much more extreme conditions can definitely cause arcing between the sample and metallic probe and lead to failure in thermocouple performance. Fibre-optic sensors can measure only up to 400 °C, whereas the dry reforming of methane reaction must be performed at the temperature of at least 700 °C. Meanwhile, although the applicable temperature range of the optical pyrometers is suited for the dry reforming of methane, it only measures the surface temperature, which differs from the interior of catalyst particles (Haque 1999; Thostenson and Chou 1999; Will et al. 2004). Moreover, even using a sensor that was known to be insensible to microwave can cause a modification of the temperature profile inside as shown in Fig. 4 (Estel et al. 2017).

The design of the microwave cavity, or applicator, is vital to ensure the efficiency in microwave heating. The distribution of temperature within the object and of the electromagnetic fields within the cavity are basically linked to each other. Consequently, it depends on the type of applicators which are classified as single mode and multi-mode. As can be seen in Fig. 5a, a, single-mode applicator in which focusing microwave field at a given location is generated is only suitable to work with small amounts of materials that need to be heated; otherwise, non-uniform temperature distribution may occur. On the other hand, a multimode applicator is capable of more even distribution; thus, it is the most common processing device used in industrial applications (Fidalgo and Menéndez 2013; Thostenson and Chou 1999). So far, there are two different designs of the multi-mode applicator, one with the turntable and one with the mode stirrer as can be seen in Fig. 5b. The turntable which is now widely used in a domestic microwave oven rotates to allow the target to contact more evenly with microwave transported from the magnetron. The applicator without a turntable uses a rotating reflector (mode stirrer) just under the outlet of a waveguide to distribute the microwave more evenly.

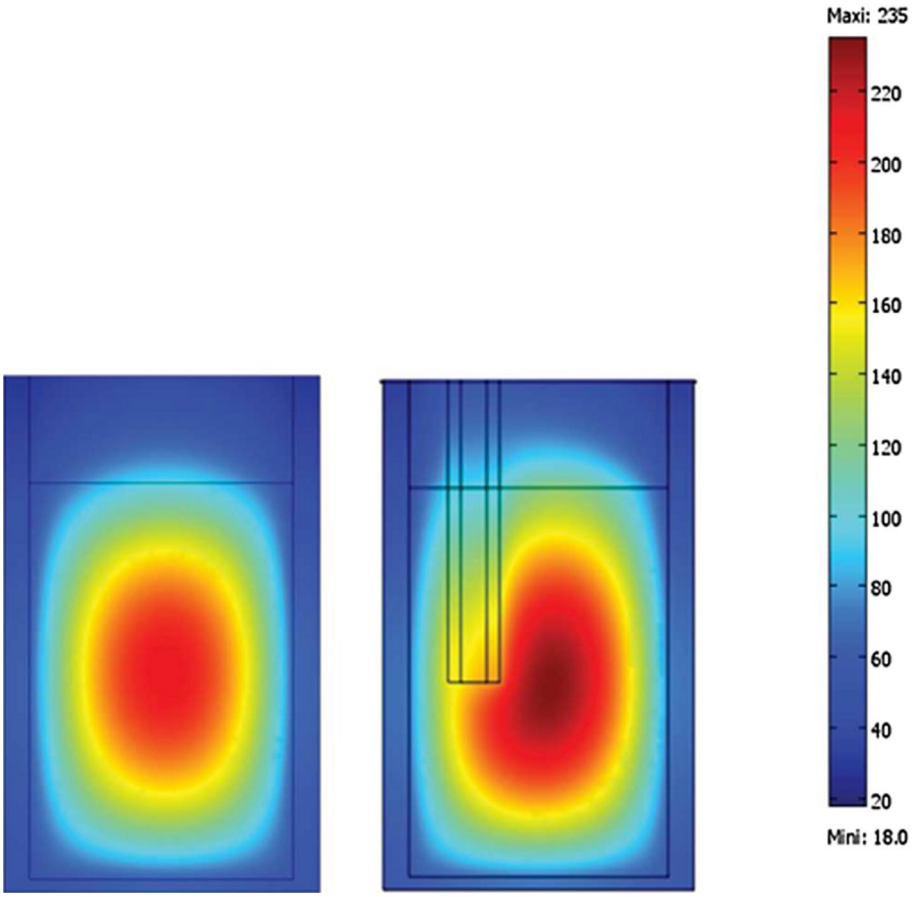

Fig. 4 Effect of inserting a temperature sensor inside the microwave cavity on the distribution of temperature. The left image is the temperature profile inside a blank cavity while the right image is the one in the presence of (right) and without (left) a temperature sensor. Reprinted from Estel et al. (2017), Copyright (2017) with permission from Elsevier

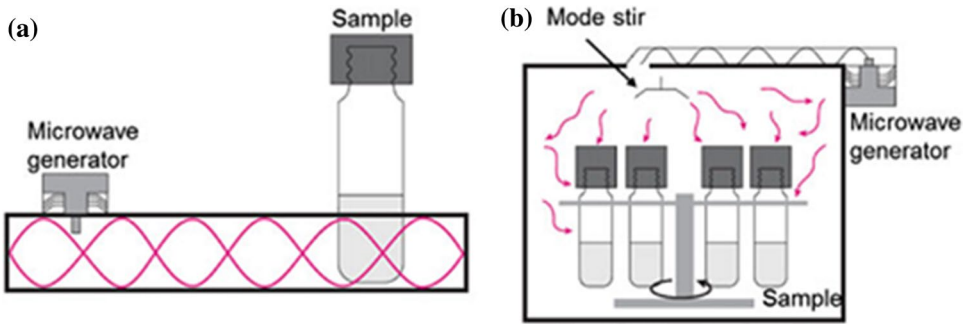

Fig. 5 Illustration of a **a** single-mode cavity and **b** multimode one. The multimode was illustrated with both the turntable and the mode stirrer. Reprinted by permission from Horikoshi et al. (2018), Copyright (2018) Springer Nature

According to Fig. 6, it is not difficult to recognize that neither applicator is perfect as there are always dead points or overheating points, although the mutimode one exhibits a more uniform distribution of electromagnetic fields. The larger frequency is applied in the same cavity or the larger cavity is used at the same frequency; the higher uniformity can be obtained. However, due to the predictable field distributions, the separated effects of electric and magnetic field components on a specific object can only be investigated in a suitable single-mode cavity (Cheng et al. 2001, 2002; Rosa et al. 2016).

Microwave-enhanced reformers

The extremely endothermic nature of the dry reforming of methane requires an accurate measurement of the reaction. However, as stated above, this task is not easy due to the challenges of microwave heating such as non-uniform temperature distribution and the risk of interaction between the electromagnetic field and the metals which must be used to make up the high-temperature thermocouples. In order to overcome this critical issue, the metal sheathed thermocouples must be protected by a microwave-transparent quartz tube and connected with a grounded filter capacitor before inserting it into the radiated catalyst bed (Li et al. 2017, 2018a, b; Zhang et al. 2018a, b, c). This method does not only help to protect the thermocouples

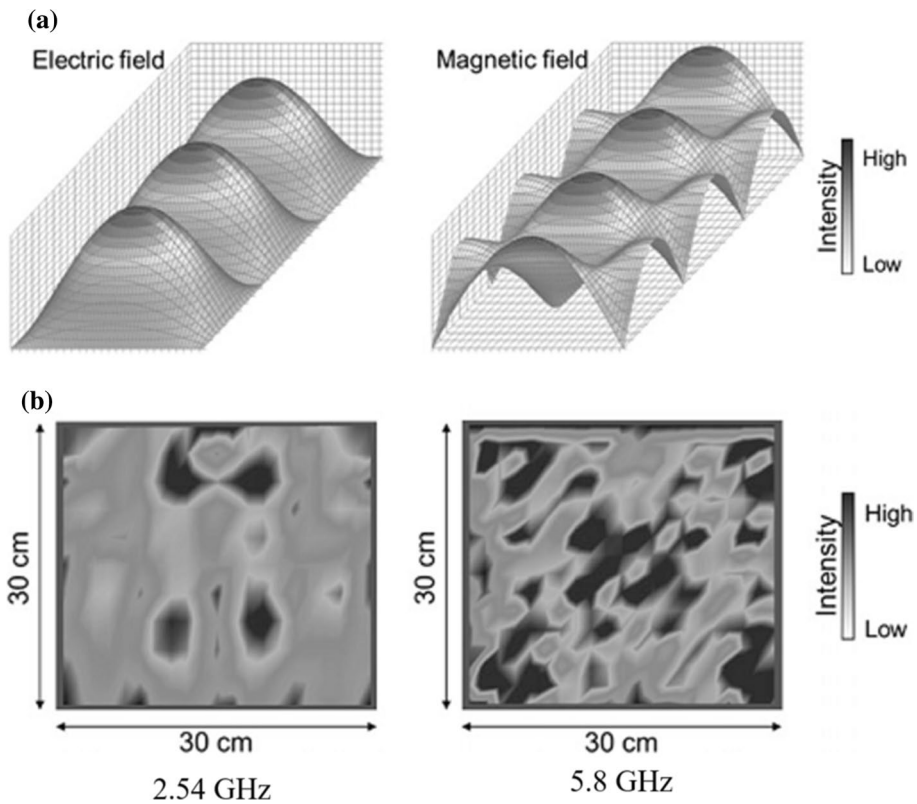

Fig. 6 Simulation of the distribution of **a** the electric and magnetic fields in a single-mode cavity, and **b** electric field in a 30 × 30 × 30 cm multimode one at 2.54 and 5.8 GHz. Electric and magnetic fields are observed to be separated from each other in a single-mode cavity, while they cannot be distinguished in a multimode one. At the same size of multimode cavity, higher frequency results greater uniformity. Reprinted by permission from Horikoshi et al. (2018), Copyright (2018) Springer Nature

from metal-microwave interaction but also eliminates the breakdown discharge and electrical noise. Recently, Gangurde et al. (2017, 2018) proposed a non-contact method for continuously monitoring of the 2D temperature distribution in a microwave-enhanced reactor by using a thermal camera. They employed both optical fibres and N-type thermocouples to measure the temperature profile along the radial direction of the reactor and temperature of the lower and upper parts of the catalyst bed for calibration. The N-type thermocouples could not be placed in the radiated regions to avoid dangers from microwave-metal interaction; thus, the single-mode cavity had to be modified as seen in Fig. 7. It was reported that hot spot generation could be detected by the thermal camera; however, using it alone does not ensure the correct measurement due to its complex dependence on many factors. Thus, at least one contact temperature sensor must be additionally employed for calibration.

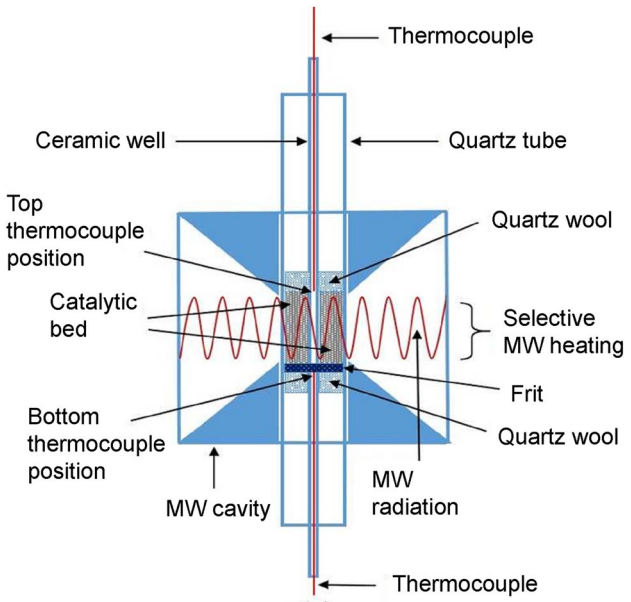

Fig. 7 Modified single-mode cavity for continuously monitoring of the 2D temperature distribution in a microwave-enhanced reactor using a non-contact thermal camera calibrated with contact thermocouples that must be placed outside the radiated regions. Reprinted with permission from Gangurde et al. (2017), Copyright (2017) American Chemical Society

Due to its excellent microwave-transparent and heat resistance properties, quartz has been used to make the reaction tube for almost microwave-enhanced reformer. Both single- and multimode applicators have been introduced for microwave-assisted DRM although the single-mode one has rarely employed due to its low energy efficiency (Fidalgo and Menéndez 2013). As shown in Fig. 8, the water sinks must be installed in front and behind of the reaction quartz tube in order to dissipate non-absorbed microwave, resulting in a lot of wasted energy in the case of using single-mode applicator (Fidalgo et al. 2008). In addition, a simulation work demonstrated that the temperature gradient in the radial direction can reach up to 210 °C (Julian et al. 2019). Practically, the rotation of the reactor was proven to be effective in reducing this gradient as shown in Fig. 9, but this modification would be very complicated (Julian et al. 2019). Consequently, the multimode applicator has been the most common choice in both laboratory-scale (Li et al. 2018a, b) and pilot-scale (Fidalgo and Menéndez 2012).

When a domestic microwave oven is utilized and modified to become a microwave-enhanced reactor, the turntable mode must be disabled due to the complex connection with outside parts as can be seen in Fig. 10. Microwave distribution is now only based on the multiple reflections from the

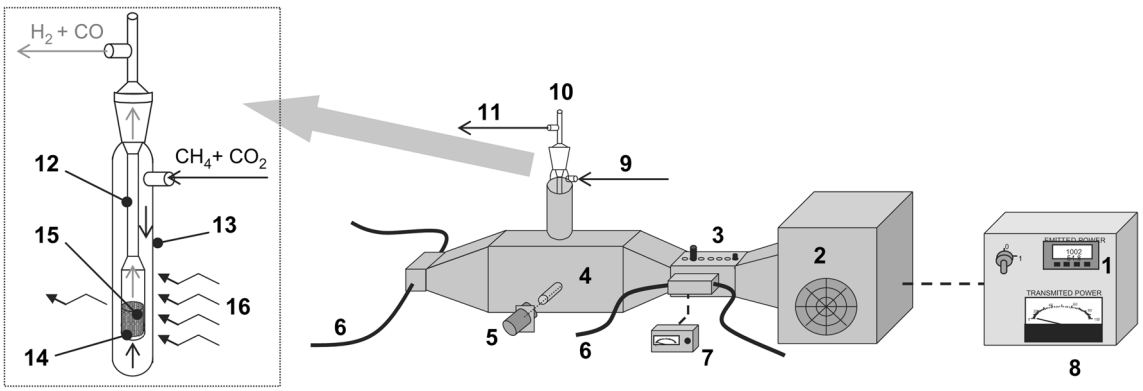

Fig. 8 Schematic drawing of the single-mode microwave-assisted DRM reactor where 1 is input power control unit, 2 is magnetron, 3 is manual two-tub unit, 4 is waveguide, 5 is optical pyrometer, 6 is water sink, 7 and 8 are reflected and transmitted power control, respectively, 9 is inflow gas line, and 10 is quartz reactor-jacket and catalyst/microwave receptor. The schematic drawing of object 10 is inserted at the left side where 11 is outflow gas line, 12 is quartz reactor, 13 is quartz jacket, 14 is porous plate, 15 is catalyst/microwave receptor bed, and 16 is microwave radiation. Reprinted from Fidalgo et al. (2008), Copyright (2008), with permission from Elsevier

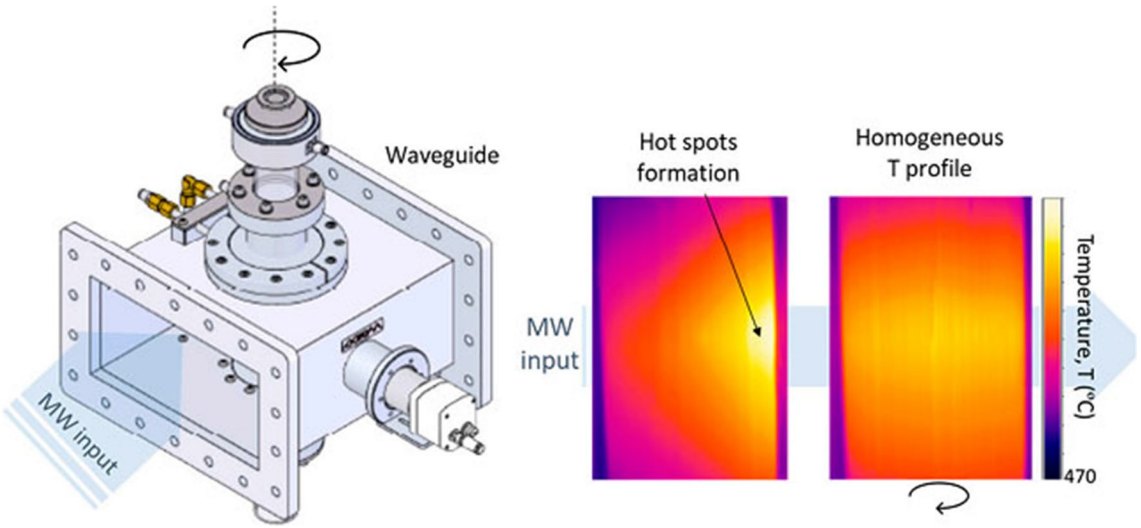

Fig. 9 Single-mode cavity coupled with rotatable reactor. Note that the temperature distribution in the cases of rotating configuration (right) is more uniform than in the case of standing (left). Adapted from (Julian et al. 2019)

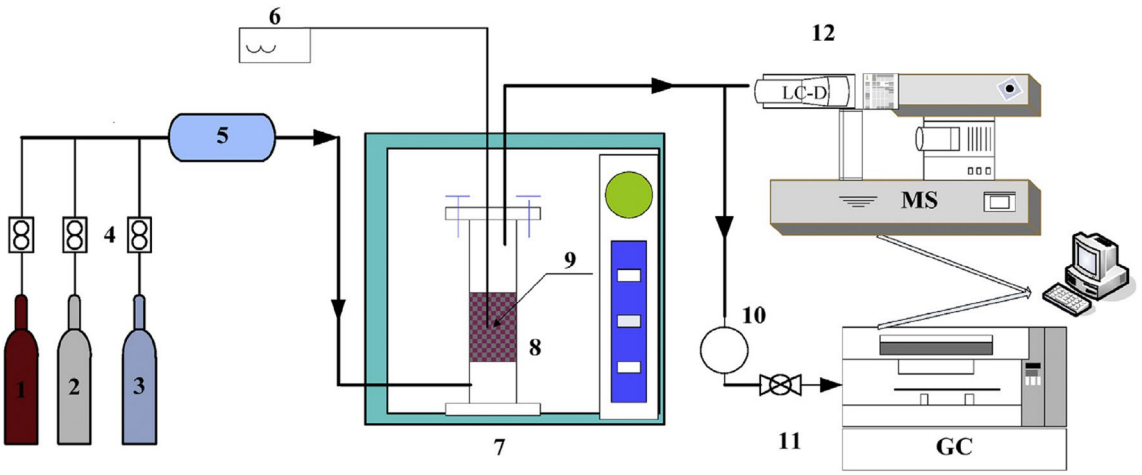

Fig. 10 Multi-mode microwave-assisted dry reforming of methane (DRM) reactor modified from domestic microwave oven where 1 to 3 are CH4, CO2 and argon cylinders, respectively, 4 are mass flow meters, 5 is gas mixing device, 6 is thermocouple, 7 is microwave oven, 8 is quartz reactor, 9 is catalyst bed, 10 is gas collecting bag, 11 is gas chromatography (GC), and 12 is mass spectrometry (MS). Reprinted from Zhang et al. (2018a, b, c), Copyright (2018), with permission from Elsevier

cavity walls, resulting in an inhomogeneous temperature profile within the catalyst bed (Li et al. 2011; Salema et al. 2013; Zhang et al. 2018a, b, c). Zhu et al. (2017) proposed a multi-physics coupling model to simulate electric field distribution inside the multi-mode applicator under normal and rotary heating. Results showed that heating uniformity can be improved significantly by a rotating microwave radiation source.

Recently, a novel design of turntable multimode microwave device, which ensures the uniform distribution of electromagnetic fields inside the applicator was successfully developed (Nguyen et al. 2019). This approach is basically the opposite of conventional design of the microwave-assisted apparatus. A household microwave oven must be placed on a tray that can rotate 360° clockwise followed by reversing the direction of rotation to the counterclockwise to not affect the outside connections. Meanwhile, a reaction flask was fixed to a central pipe, which is extended outside the microwave oven through a port and fixedly attached to the support frame as illustrated in Fig. 11. Consequently, the magnetron was rotated around the fixed flask allowing the target to be contacted evenly with microwave generated. The port was covered by a metal tube according to the instructions of Mingos and Baghurst (1991), resulting in a

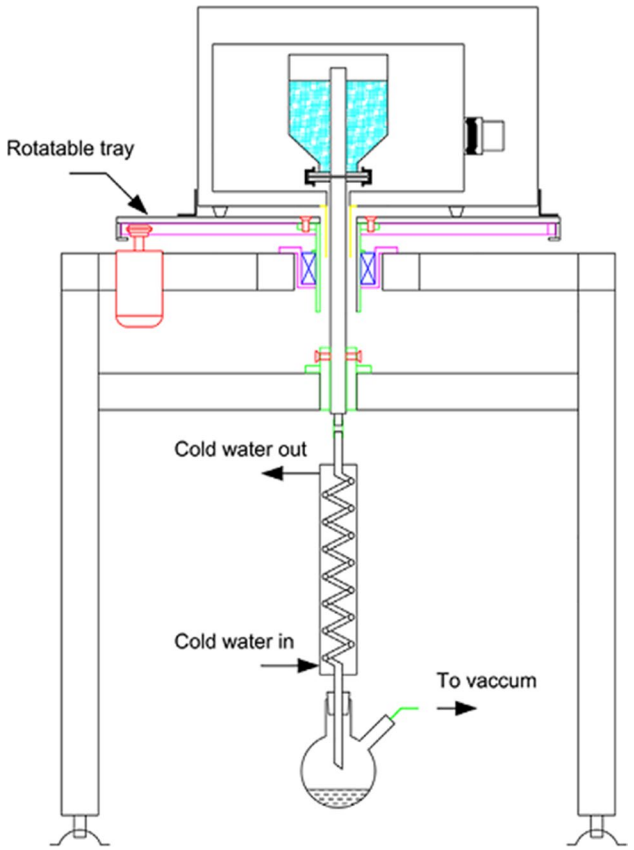

Fig. 11 Turntable multimode microwave device for solvent-free extraction of essential oil. Note that the setup was developed from a household microwave oven so that the magnetron can be rotated around the fixed flask resulting in a uniform distribution of electromagnetic field. Reprinted with permission from (Nguyen et al. 2019), Copyright (2019) John Wiley and Sons

low microwave leakage that was reported to be below the safety limit of 5 mW/cm^2 (Schiffmann and Steiner 2012). Although the modified setup was originally employed for the solvent-free microwave-assisted extraction, it can be practically developed to a novel microwave-enhanced reformer in the future.

Catalysts

Since microwave-assisted DRM requires microwave irradiation as the thermal source to drive the endothermic reaction, the degree of microwave interaction governed by the dielectric attributes of materials related to the corresponding structural and physical features is crucial (Hamzehlouia et al. 2018). However, various gaseous materials possess intrinsic dielectric properties that are not appreciably favouring the microwave interaction. From the above reasons, the exploration and development has been mainly focused on the solid material, namely catalyst and microwave receptor (C/MR), which can act as a catalyst for reforming reaction and simultaneously dissipate the absorbed microwave irradiation to thermal energy in the form of heat for microwave-assisted DRM (Fidalgo et al. 2008; Hamzehlouia et al. 2018). Hence, apart from the ability of resistance towards the carbonaceous deposition and metal sintering on catalyst surface, the catalyst and microwave receptor performance for improving the conversion of microwave radiation to heat source depending on types of microwave-absorbing material used is also essential.

The general catalysts employed in microwave-assisted DRM are similar to methane dry reforming, including noble metal catalyst, i.e. Pt- and Ru-based catalyst (Gangurde et al. 2018; Zhang et al. 2003) and non-noble metal catalysts (i.e. Ni- and Fe-based catalyst) (Odedairo et al. 2016; Zhang et al. 2018a, b, c; Herminio et al. 2020; Qin et al. 2020) as their mechanisms are fundamentally alike. However, considering the microwave selective heating mechanism governs the reforming performance, microwave-absorbing materials with significant dielectric properties are extensively investigated as catalyst for microwave-assisted DRM. Additionally, numerous studies about the development of novelty catalyst, such as coating or mixing metal catalysts with microwave-absorbing materials, have recently conducted to enhance the reforming performance with low carbonaceous deposits and excellent energy conversion of microwave irradiation to heat generation. The performance of catalyst and microwave receptor reported in literature is summarized in Table 5.

Carbon-based catalysts

In heterogeneous catalysis systems, carbon-containing materials, i.e. carbon blacks, activated carbon and chars from biomass residues, are widely evaluated as support or as catalyst in reactions due to their thermal durability, availability, great porosity, low cost and oxygen surface groups improving the catalytic performance and product selectivities (Rodriguez-Reinoso 1998; Titirici et al. 2015; Balajii and Niju 2019; Hassan et al. 2020). Particularly, in comparison with metal-based catalysts, carbon-based catalysts possess excellent ability in microwave absorption, known as good microwave receptors appropriate for microwave-assisted DRM (Fidalgo et al. 2010; Li et al. 2017). Since the degree of microwave interaction to produce heat is highly reliant on type of microwave-absorbing materials, several parameters including dielectric constant, loss tangent and loss factor are employed to measure the strength of their dielectric attributes, where dielectric constant (ε') and loss factor (ε'') represent the corresponding capability of material in absorption of electromagnetic wave and the capability of material for dissipating the absorbed wave into heat), whereas loss tangent ($\tan\delta$) is the $\varepsilon''/\varepsilon'$ ratio describing the efficiency of the absorbed microwave convert into thermal energy (Hamzehlouia et al.

Table 5 Catalytic performance of different catalysts recently applied in microwave-assisted dry reforming of methane (DRM)

Catalysts and microwave receptors (C/MR)	CH_4/CO_2 ratio	T (°C)	VHSV ($ml\ g_{cat}^{-1}\ h^{-1}$)	TOS (min)	Reforming performance			References
					CH_4 conversion (%)	CO_2 conversion (%)	H_2/CO ratio	
Carbon-based catalysts								
Char[a]	1/1	800	332	120	82	98	0.66	Domínguez et al. (2007a, b)
Activated carbon (filtracarb FY5)	1/1	800	320	300	70	79	0.80	Fidalgo et al. (2008)
FY5	1.2/1	800	290	150	60	80	–	Fidalgo et al. (2010)
BPL	1/1	800	320	150	10	7	–	Fidalgo et al. (2010)
CQ	1/1	800	680	150	1	6	–	Fidalgo et al. (2010)
Activated carbon (FY5–63)[b]	1/1	800	320	300	65	91	–	Fidalgo et al. (2010)
Activated carbon (FY5ox)[c]	1.2/1	800	290	150	13	3	–	Fidalgo et al. (2010)
Bio-char[d]	1/1	800	1200	120	12	4	–	Fidalgo et al. (2008)
Metal-based catalysts								
40%Ni/CeO_2	1/1	850	10,200	840	68	–	1.47	Odedairo et al. (2016)
2%Cr–40%Ni/CeO_2	1/1	850	10,200	840	76	–	1.45	Odedairo et al. (2016)
2%Ta–40%Ni/CeO_2	1/1	850	10,200	840	74	–	1.47	Odedairo et al. (2016)
2%Fe–40%Ni/CeO_2	1/1	850	10,200	840	71	–	1.40	Odedairo et al. (2016)
4%Fe/Al_2O_3–SiC	1/1	750	1200	–	63	59	0.93	Zhang et al. (2018a, b, c)
8%Fe/Al_2O_3–SiC	1/1	750	1200	–	87	88	0.96	Zhang et al. (2018b)
12%Fe/Al_2O_3–SiC	1/1	750	1200	–	93	92	0.98	Zhang et al. (2018b)
16%Fe/Al_2O_3–SiC	1/1	750	1200	–	89	90	0.96	Zhang et al. (2018b)
$Ni_{0.491}Mg_{0.258}Al_{0.250}O$	1/1	600	120,000	600	38	51	1.08	Ojeda-Niño et al. (2019)
$Ni_{0.429}Mg_{0.286}Al_{0.286}Pr_{0.005}O$	1/1	600	120,000	600	44	57	1.18	Ojeda-Niño et al. (2019)
$Ni_{0.433}Mg_{0.289}Al_{0.278}Pr_{0.025}O$	1/1	600	120,000	600	38	52	1.10	Ojeda-Niño et al. (2019)
$Ni_{0.550}Mg_{0.212}Al_{0.238}Pr_{0.055}O$	1/1	600	120,000	600	50	61	1.25	Ojeda-Niño et al. (2019)
Mixing metal catalysts with microwave-absorbing materials								
FY5 + Ni/Al_2O_3	1/1	800	1500	180	90	98	–	Fidalgo et al. (2011)
CQ + Ni/Al_2O_3	1/1	800	1500	180	84	92	–	Fidalgo et al. (2011)
Ni/FY5	1/1	800	1500	180	85	100	–	Fidalgo et al. (2011)
FY5 + eFe[e]	1/1	800	680	160	72	93	–	Bermudez et al. (2012)
CQ + eFe[e]	1/1	800	680	160	42	70	–	Bermudez et al. (2012)
5%Ni/bio-char[d]	1/1	800	1200	120	83	87	–	Li et al. (2017)
10%Ni/bio-char[d]	1/1	800	1200	120	84	89	0.54	Li et al. (2017)
15%Ni/bio-char[d]	1/1	800	1200	120	80	89	–	Li et al. (2017)
20%Ni/bio-char[d]	1/1	800	1200	120	79	88	–	Li et al. (2017)
Char + Na	1/1	975	2400	–	73	93	–	Li et al. (2018a, b)
Char + K	1/1	975	2400	–	73	92	–	Li et al. (2018a, b)
Char + Ca	1/1	975	2400	–	79	83	–	Li et al. (2018a, b)
Char + Mg	1/1	975	2400	–	80	82	–	Li et al. (2018a, b)
Char + Ni	1/1	975	2400	–	87	93	–	Li et al. (2018a, b)
5%Fe–C	1/1	900	7200	20	95	99	1.01	Li et al. (2019)
10%Fe–C	1/1	900	7200	20	98	100	1.02	Li et al. (2019)
20%Fe–C	1/1	900	7200	20	93	100	0.93	Li et al. (2019)

CQ metallurgical coke, *BPL* bituminous coal-based activated carbon, *FY5* coconut shell-derived activated carbon, *VHSV* volume hourly space velocity

[a]Char was compose of ash (24.4 wt%), volatile matter (12.3 wt%) and fixed carbon (63.3 wt%)

[b]Coconut shell-derived activated carbon (FY5) after CO_2 activation up to a burn-off degree of 63%

[c]Coconut shell-derived activated carbon (FY5) after oxidation in $(NH_4)_2S_2O_8/H_2SO_4$ solution

[d]Bio-char was made of K (36.4 wt%), Fe (9.04 wt%), Ca (11.37 wt%), Mg (13.12 wt%), Al (14.43 wt%) and Na (15.64 wt%)

[e]Fe-rich steel-making slag (eFe) was composed of CaO (41.7 wt%), Fe_2O_3 (21.7 wt%), SiO_2 (15.0 wt%), MgO (3.7 wt%), MnO (3.5 wt%) and Al_2O_3 (2.3 wt%)

2018; Menéndez et al. 2010). Table 4 summarizes the dielectric attributes of recent reported carbon materials.

In the study of electric heating and microwave heating dry reforming of methane over the char produced from coffee hulls via pyrolysis, Domínguez et al. (2007a, b) found that microwave heating approach significantly enhanced the CH_4 and CO_2 conversions by achieving 82% and 98%, respectively (Domínguez et al. 2007a, b). However, a noticeable reduction in CH_4 conversion was observed for microwave heating case after few minutes indicating the severe blockage of active sites by carbonaceous species, carbon nanofibres as evident by scanning electron microscopy (SEM) analyses (Fig. 12). Interestingly, unlike the trend observed for CH_4 conversion, the CO_2 conversion consistently maintained at around of 98% with time-on-stream due to the high potassium content (40.3 wt%) existed in char catalysing the carbon gasification reaction at high reaction temperature. From the above results, a 2 steps reaction pathways were proposed for microwave-assisted DRM, in which CH_4 decomposition (Eq. 10) followed by carbon gasification by CO_2 where the carbon source was reportedly not only originated from CH_4 (Eq. 11) but also contributed by the certain type of carbon content presented in the char catalyst (Eq. 12) (Domínguez et al. 2007a, b).

$$CH_4 \rightarrow C + 2H_2 \tag{10}$$

$$C_{(CH_4)} + CO_2 \rightarrow 2CO \tag{11}$$

$$C_{(Char)} + CO_2 \rightarrow 2CO \tag{12}$$

To investigate the influence of various carbon materials on microwave-assisted DRM performance, Fidalgo et al. (2010) had synthesized metallurgical coke (CQ) and various activated carbons, including bituminous coal-based activated carbon (BPL), coconut shell-derived activated carbon (FY5), as well as FY5s prepared with various conditions such as activated carbon (FY5–63) and activated carbon (FY5ox), as given in Table 5. The reactant conversions declined in the following order activated carbon (FY5–63) > coconut shell-derived activated carbon (FY5) > activated carbon (FY5ox) > bituminous coal-based activated carbon (BPL) > metallurgical coke (CQ) catalysts. From the study, they discovered that catalytic performance of carbon

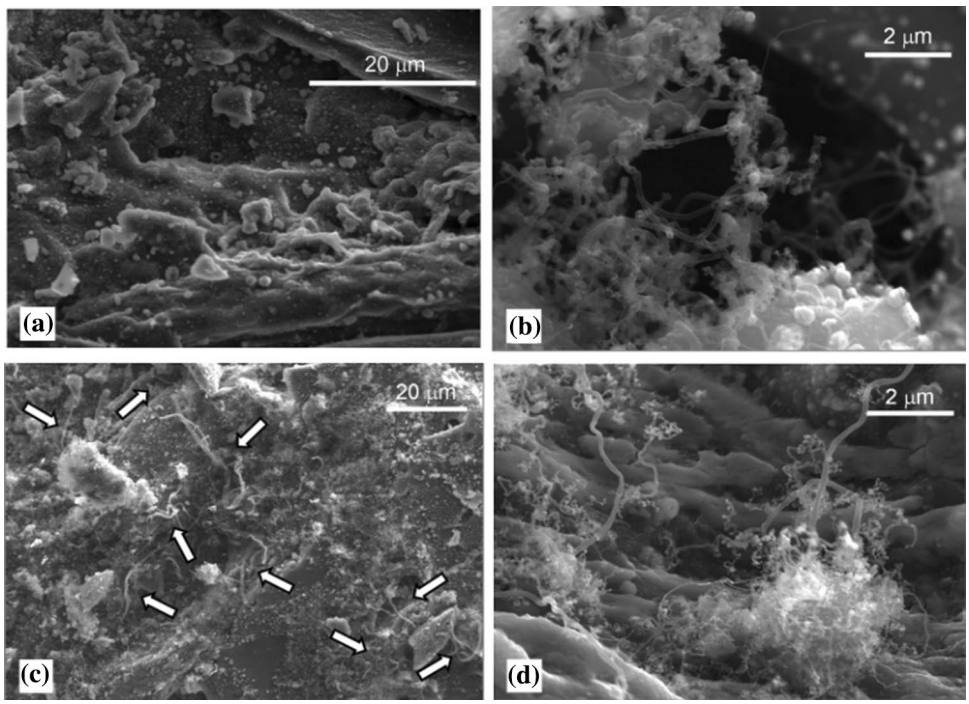

Fig. 12 Scanning electron microscopy (SEM) micrographs of chars after reactions for 2 h-on-stream at temperature of 800 °C: **a** deposited coke on char surface after methane cracking in electrical heating; **b** nanofibres after CH_4 cracking in microwave heating; **c** surface of char after dry reforming of methane in microwave heating (arrows point at nanofibres location); **d** nanofibres after dry reforming of methane in microwave heating. The deposition of carbon nanofibres inevitably grows on char surface, as a result of accelerated CH_4 decomposition under the employment of microwave heating dry reforming of methane even though this approach appreciably improves the catalytic activity. This is the main factor leading to the catalyst deactivation within minutes due to severe clogging of active sites of the char. Reprinted with permission from Domínguez et al. (2007a, b). Copyright (2007) American Chemical Society

materials associated with microwave selective heating mechanism crucially depended on their oxygen surface groups and porosity. Amongst carbonaceous materials employed, coconut shell-derived activated carbon possessed the highest reactant conversion owing to its excellent microporosity capturing the CO_2 reactants. Interestingly, oxidized activated carbon (FY5ox) owned a similarly micropores as coconut shell-derived activated carbon, but it did not favour microwave-assisted DRM performance under microwave assistance. Fidalgo et al. (2010) assigned this behaviour to the difficulty in the dissipation of adsorbed microwave into thermal energy due to the presence of electronegative oxygen restraining their mobility for promoting microwave heating (Fidalgo et al. 2010). Theoretically, during microwave heating, the delocalized π-electrons of carbon materials prone to pair the electric component phase changes associated with electromagnetic field for heat dissipation (Fig. 13). However, oxygen surface groups from oxidized materials are electron-withdrawing resulting in a restriction to the mobility of partial π-electrons and hence, confining the heat dissipation (Hashisho et al. 2009; Fidalgo et al. 2010).

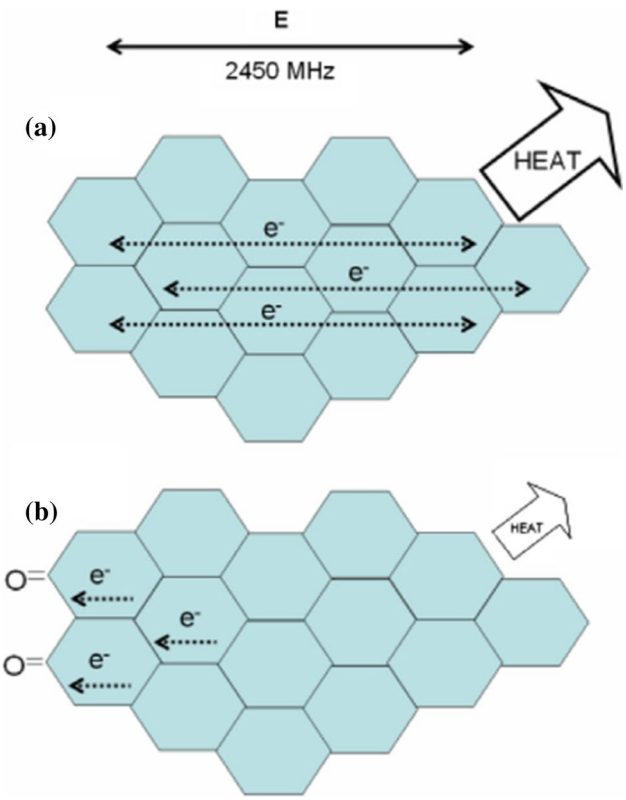

Fig. 13 Effects in microwave heating of carbonaceous materials: **a** microwave heating induced by the Maxwell–Wagner effect (Interfacial polarization), the delocalized p-electrons pairing electric component phase changes of the electromagnetic field's heat dissipation; **b** oxygen surface groups are electron-extracting which restrain the movement of partial p-electrons of the basal planes and thus limiting dissipation of heat. This theory explains the disparity in catalytic performance of different carbon materials associated with their corresponding oxygen surface groups and porosity, which impactfully affect their microwave selective heating mechanism in the degree of conversion of adsorbed microwave into thermal energy for microwave-assisted dry reforming of methane (DRM). Reprinted from (Fidalgo et al. 2010), Copyright (2010), with permission from Elsevier

Metal-based catalysts

Similar to common the dry reforming of methane, the employment of metals for easing the CH_4 activation, improving dispersion of hosting metal and hindering the metal agglomeration and sintering plays an essential role in microwave-assisted DRM process with respect to stability, reactant conversions and product selectivity. Evaluation of a series of metals for microwave-assisted DRM has been conducted based on their inherent nature and numerous main selection criterions. As reported in literature, since formation of carbonaceous species is inevitable in microwave-assisted DRM and carbon is also known as a good microwave receptor, addition of several metals could enhance the dispersion of hosting metal and simultaneously promote the carbon formation accelerating the microwave selective heating mechanism (Odedairo et al. 2016).

In the investigation of metal impact on Ni/CeO_2 catalysts for microwave-assisted DRM, Odedairo et al. (2016) prepared three different Ni catalysts promoted by several metals, namely, $2\%Ta\text{-}40\%Ni/CeO_2$, $2\%Cr\text{-}40\%Ni/CeO_2$ and $2\%Fe\text{-}40\%Ni/CeO_2$ via co-impregnation approach (Odedairo et al. 2016). The incorporation of Ta and Cr to Ni/CeO_2 catalysts reportedly inhibited NiO agglomeration and increased reducibility of Ni catalysts owing to strengthened interaction between support and metal during synthesis. The CH_4 conversion in microwave-assisted DRM followed the order: $2\%Cr\text{-}40\%Ni/CeO_2 > 2\%Ta\text{-}40\%Ni/CeO_2 2\%Fe\text{-}40\%Ni/CeO_2 > Ni/CeO_2$. In fact, the structure of carbon formed during microwave-assisted DRM also has a substantial impact on the reforming activity. Transmission electron microscopy (TEM) results confirmed the presence of multi-walled carbon nanotubes/layered graphene composite (M/GR) on $2\%Cr\text{-}40\%Ni/CeO_2$ (Fig. 14) while multi-walled carbon nanotubes/cup-stacked carbon nanotubes composite (M/CSCNT) and multi-walled carbon nanotubes/graphitic nanofibre/graphene (3-phase composite) were found on $2\%Ta\text{-}40\%Ni/CeO_2$ (Fig. 15) and $2\%Fe\text{-}40\%Ni/CeO_2$ (Fig. 16), respectively after reaction. Amongst the catalysts, $2\%Cr\text{-}40\%Ni/CeO_2$ possessed the most graphene content on its surface. According to Menéndez et al. (2010), graphene owns plentiful of sp^2 π electrons that able to absorb microwave effectively and transform the subsequent absorbed microwave into microplasmas or hot spots (Menéndez et al. 2010). Hence, Odedairo et al. (2016) suggested that the good catalyst activity of Cr- and Ta-doped catalysts could

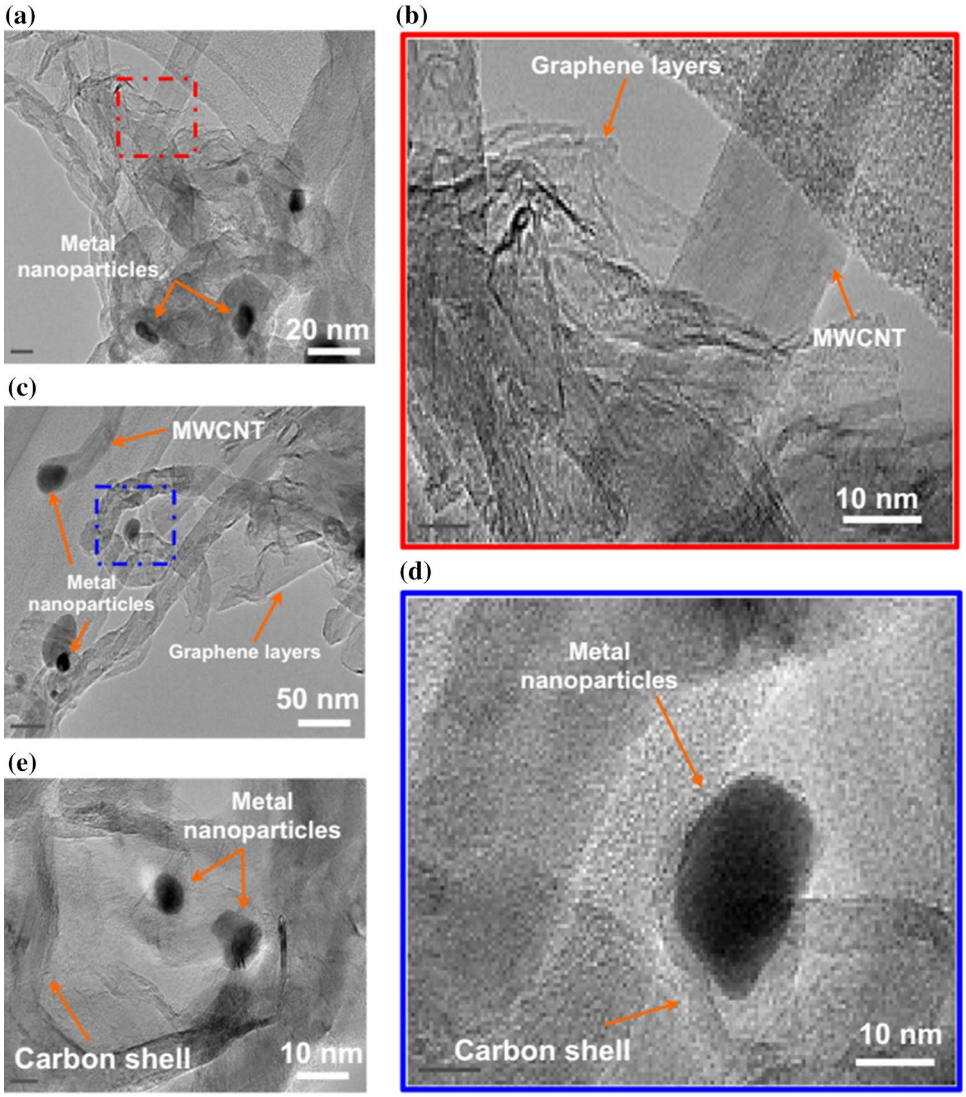

Fig. 14 Transmission electron microscopy (TEM) images of multi-walled carbon nanotubes/layered graphene (M/GR) obtained on 2%Cr–40%Ni/CeO_2 after 14 h-on-stream reaction. The graphene and multi-walled carbon nanotubes and metal nanoparticles are evidently dispersed on the transparent and wrinkled layered graphene and multi-walled carbon nanotubes. Graphene was crumpling into many overlapped regions owing to the strong Van der Waals interactions amongst layers. The metal nanoparticles are found at the tip of a multi-walled carbon nanotube and coated with carbonaceous shell could be a result of the CH_4 decomposition. Reprinted from Odedairo et al. (2016), Copyright (2015), with permission from Elsevier

be attributed to the in situ grown graphene on catalyst surface which sustainably released heat to the neighbouring Ni particles under microwave irradiation and thus, facilitating the microwave selective heating mechanism for microwave-assisted DRM process (Odedairo et al. 2016).

Zhang et al. (2018b) assessed the factors, i.e. catalyst carriers, microwave power, active component contents and space velocity, affecting catalytic performance of Al_2O_3–SiC supported catalysts for microwave-assisted DRM. They found that an increase in active Fe content rapidly enhanced the catalytic activity from Fe loading of 4–12 wt% but an insignificant decline in catalytic activity was discerned at Fe content of 16 wt%. With the optimal content of Fe (12 wt%), the highest CO_2 and CH_4 conversion about of 92% and 93% were achieved. As reported by Zhang et al. (2018b), active Fe component below 12 wt% was insufficient to disperse finely over the whole support surface providing sufficient active sites for microwave-assisted DRM while Fe content above 12 wt% easily led to metal sintering at high temperature. In contrast with the discussion of Zhang et al. (2018b), Odedairo et al. (2016) suggested that carbon deposit was indeed active in the existence of microwave irradiation but it was also favourable to the side reactions causing a drop in reforming performance (Zhang et al. 2018b).

In the study of microwave-assisted DRM activity with respect to the stability, Ojeda-Niño et al. (2019) found that the incorporation of Pr not only significantly enhance the thermal stability for the Ni–Mg–Al catalysts at high-temperature microwave-assisted DRM but also promote the CO_2 adsorption in a capture-release reversible dynamic depending on the basicity strength. Overall, they discovered that the Pr loading did not has a direct correlation

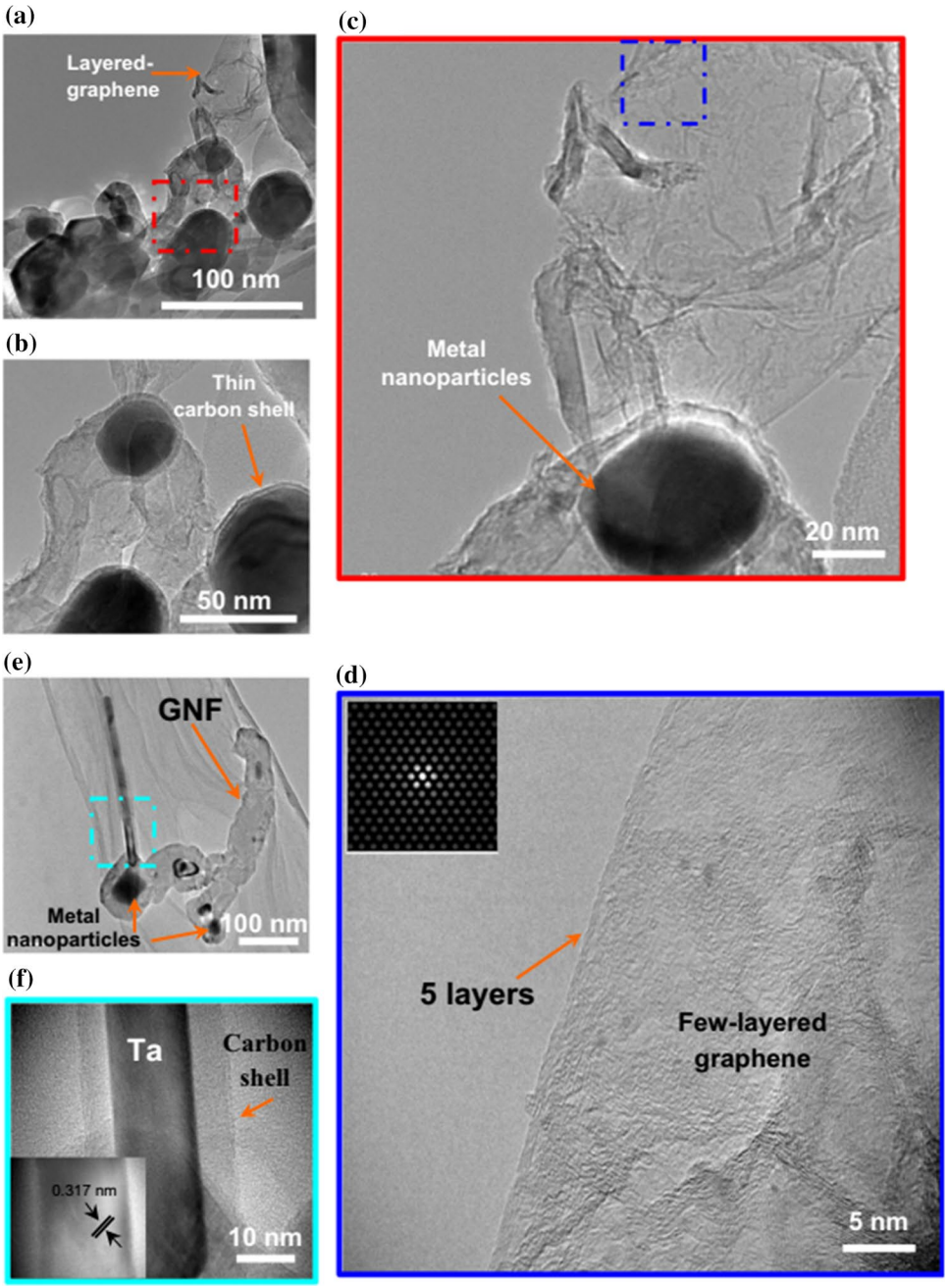

Fig. 15 Transmission electron microscopy (TEM) images of multi-walled carbon nanotubes/graphitic nanofibre/layered graphene (3-phase composite) obtained on 2%Ta–40%Ni/CeO_2 after 14 h-on-stream reaction. Graphene layers with metal nanoparticles encapsulated by carbon shell can be observed. This is probably due to the nucleation of crystalline carbon forming the multi-walled carbon nanotubes which catalysed by Ni particles. Reprinted from Odedairo et al. (2016), Copyright (2015), with permission from Elsevier

towards the catalytic performance for the reaction but it considerably influences catalytic stability. With respect to the resistibility towards carbon formation, Pr reportedly improved the dispersity of metallic Ni particles resulting in the reduction of their particle sizes on catalyst surface and thus, suppressing the growth of carbonaceous deposits and metal sintering. As a result, the increasing Pr loading led to a decline in ratio of H_2 to CO due to the facilitated gasification process of carbon producing a CO-rich atmosphere.

Mixing metal catalysts with microwave-absorbing materials

Since microwave-assisted DRM process is a heterogeneous catalytic reaction involving conventional reaction mechanism and concomitant presence of microwave selective heating mechanism, the synergistic effect of mixture comprising of carbon materials and active metals for novel microwave-assisted DRM catalyst is significantly important for maximizing catalytic activity, stability and product yields at extreme operating conditions.

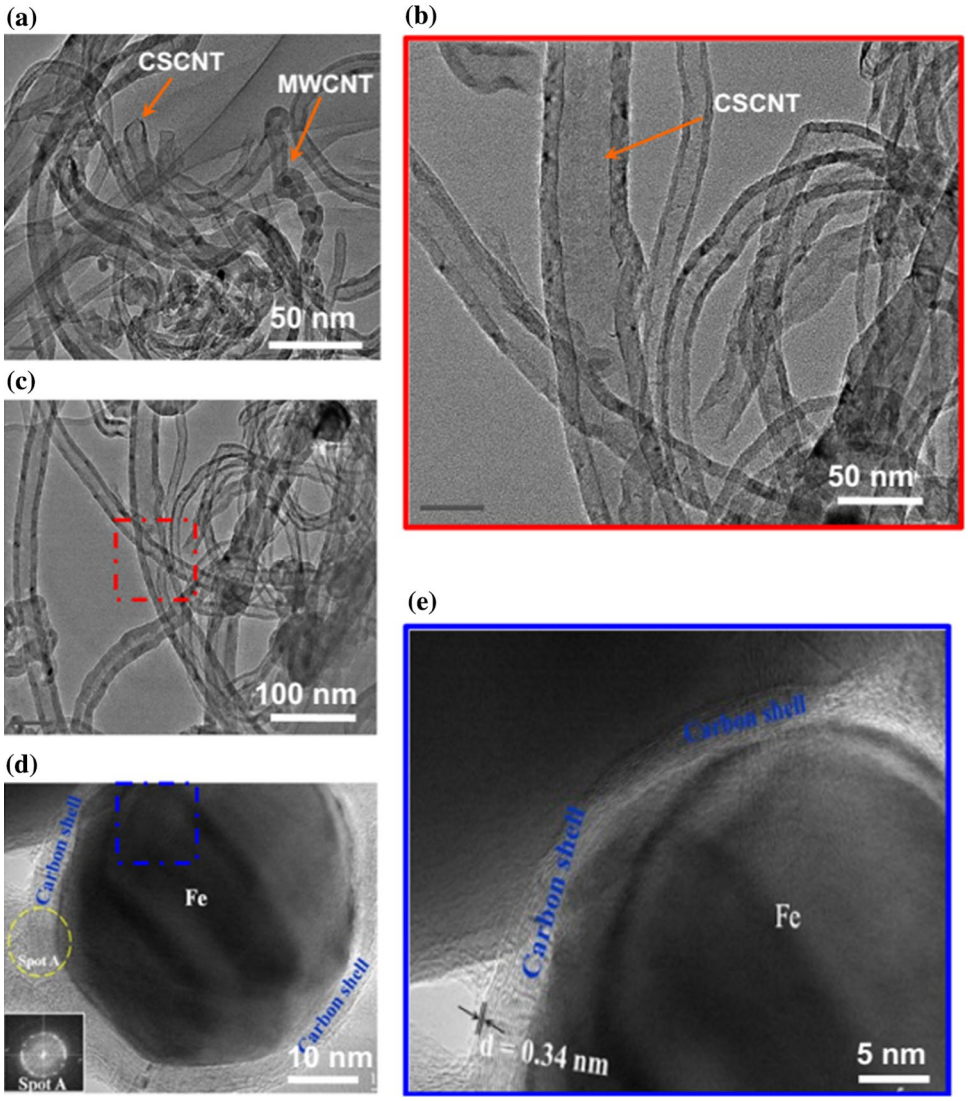

Fig. 16 Transmission electron microscopy (TEM) images of multi-walled carbon nanotubes/cup-stacked carbon nanotubes (M/CSCNT) obtained on 2%Fe–40%Ni/CeO_2 after 14 h-on-stream reaction. The cup-stacked carbon nanotubes have various sizes and lengths with large hollow tubular structure and open ends, which can continuously grow via decomposition of carbon-containing gases on a metal catalyst. Since Fe reportedly produces tubular carbon nanofibres, the formation of multi-walled carbon nanotubes/cup-stacked carbon nanotubes on 2%Fe–40%Ni/CeO_2 is predictable. Reprinted from Odedairo et al. (2016), Copyright (2015), with permission from Elsevier

In the investigation of microwave-assisted DRM performance over different carbon-mixed Ni/Al_2O_3 catalysts, Fidalgo et al. (2011) reported that coconut shell-derived activated carbon + Ni/Al_2O_3 exhibited greater reactant conversions in comparison with that of metallurgical coke (CQ) + Ni/Al_2O_3 under microwave irradiation owing to its greater dielectric properties promotes microwave heating process (Fidalgo et al. 2011). Apart from dielectric properties of material employed, poor microporosity of metallurgical coke (CQ) was also one of the key elements contributed to low catalytic performance of metallurgical coke (CQ) + Ni/Al_2O_3. Additionally, Ni/coconut shell-derived activated carbon (FY5) was synthesized to further examine the synergistic influence of coconut shell-derived activated carbon (FY5) support and metallic Ni phase on microwave-assisted DRM and Fidalgo et al. (2011) noticed that reactant conversions achieved by Ni/coconut shell-derived activated carbon (FY5) were superior and more stable than that of coconut shell-derived activated carbon (FY5) alone. However, Ni/coconut shell-derived activated carbon (FY5) exhibited a lower CH_4 conversion in comparison with coconut shell-derived activated carbon (FY5) + Ni/Al_2O_3 possibly owing to the aggregation of Ni particles and active sites clogging induced by deposited carbon. From the results, for carbonaceous material + Ni/Al_2O_3, Fidalgo et al. (2011) suggested that formation of spinel associated with metallic Ni form and Al_2O_3 support was responsible for the inhibition of Ni sintering and carbon formation, leading to good catalytic performance.

The promotional effects of different carbonaceous species, i.e. metallurgical coke (CQ) and coconut shell-derived activated carbon (FY5), on the catalytic performance of steel-making slag (eFe) catalysts for microwave-assisted DRM were evaluated by Bermudez et al. (2012) at 800 °C and the stoichiometric feed composition. Comparable to the findings of Fidalgo et al. (2011), they found that mixture of

steel-making slag (eFe) and coconut shell-derived activated carbon (FY5) exhibited greater and steadier catalytic activity with time-on-stream compared to those attained using activated carbon alone. Bermudez et al. (2012) also conducted microwave-assisted DRM over a mixture of carbon + steel-making slag and carbon + Ni/Al_2O_3 at various VSHV in order to examine their catalytic activity with different metals. They discovered that the reactant conversions over carbon + Ni/Al_2O_3 catalyst was independent from VSHV. This catalyst mixture could surprisingly achieve reactant conversions approximate to 100% with the increasing VSHV up to sixfold than that employed for activated carbon alone (Bermudez et al. 2012).

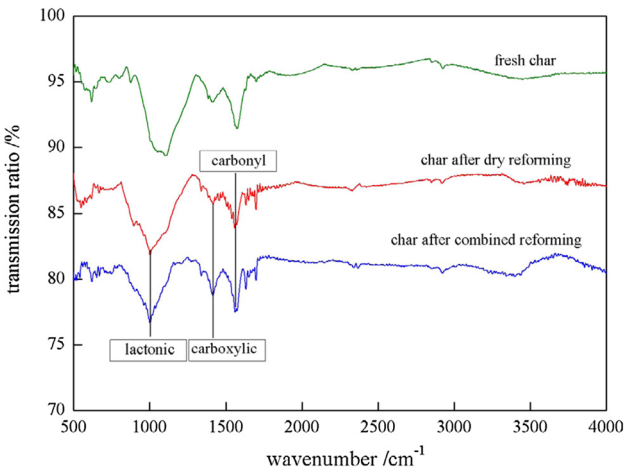

Fig. 17 Fourier transform infrared spectroscopy (FTIR) spectra of biochar before and after reaction. The detection of carbonyl and carboxylic groups confirm the presence of carbonaceous deposits on the char surface after reaction, which is responsible for the active site blockage of bio-char catalyst and hence resulting in the poor reforming activity. Reprinted from Li et al. (2016), Copyright (2016), with permission from Elsevier

Li et al. (2017) prepared the Ni/bio-char catalysts with varying Ni loading of 0–20 wt% to study the synergetic influence on their catalytic performance for microwave-assisted DRM at temperature of 800 °C (Li et al. 2017). The addition of Ni (from 0 to 20 wt%) could significantly enhance the bio-char's catalytic performance and the optimal value was achieved at 10% Ni/bio-char respecting reactant conversions and catalytic stability. With the employment of Ni loading at 10 wt% and below, the equilibrium between carbon consumption and carbon deposition rate could be achieved, and hence, recovery of active sites led to higher CH_4 conversion and better stability (Li et al. 2017). While the Ni/bio-char with Ni loading beyond 10 wt% experienced severe deactivation probably due to the active site blockage induced by metal sinterization and deposition of carbonaceous species, as evidenced by the post-reaction Fourier transform infrared spectroscopy (FTIR, Fig. 17) and scanning electron microscopy (SEM, Fig. 18) measurements. It is worth noting that the conversion of CO_2 was always greater than CH_4 and the decrease in CO_2 conversion was insignificant with growing Ni loading. This behaviour was possibly due to the gasification of carbon presented in bio-char and the reverse water–gas shift. From this study, Li et al. (2017) found that in the process of the carbon removal with CO_2, the activeness of carbon from bio-char was much higher than carbon deposits in accordance with Fidalgo et al. (2008).

Apart from transition metal-based catalyst, Li et al. (2018a, b) had prepared several alkaline metal-based catalysts and assessed their catalytic performance for microwave-assisted DRM. Interestingly, the advantages of employing alkaline metal were pronounced to the improvement in CO_2 conversion, indicating the enhancement in

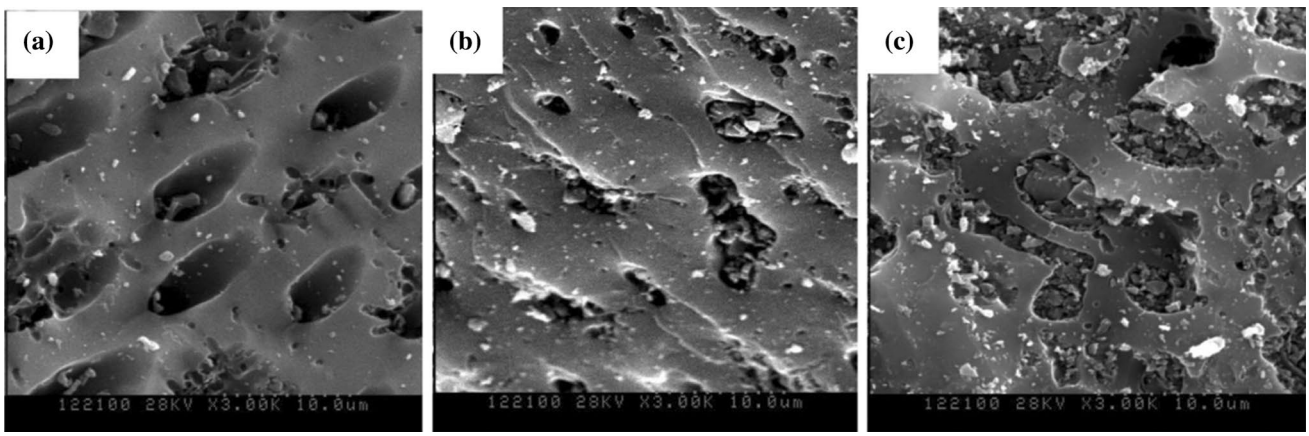

Fig. 18 Scanning electron microscopy (SEM) micrographs of the fresh and spent bio-char (**a** fresh char; **b** char after combined reforming; **c** char after dry reforming). The porosity of bio-char is evidently blocked and deposited by carbonaceous species, which is the main factor causing the rapid loss in catalytic activity of bio-char during reaction. Reprinted from Li et al. (2016), Copyright (2016), with permission from Elsevier

gasification of carbonaceous deposits possibly owing to the extent of alkalinity of catalyst. In comparison with original bio-char, the embedment of K and Na improved the conversion of CO_2 by 10.8 and 12.1%, respectively, while the embedment of Mg and Ca unexpectedly promote the rate of CH_4 decomposition. Considering the economic feasibility, applicability and availability, Li et al. (2019) continuously study the microwave-assisted DRM process over the Fe-rich biomass-derived chars. They found that Fe addition appreciably enhance the activity of methane reforming compared to original char. However, at Fe content beyond 10%, a drop in CH_4 conversion was observed owing to the metal sintering at higher temperature. Conversely, the CO_2 conversion was unaffected over different Fe content bio chars. This behaviour was attributed to the acceleration of both gasification of carbon and reverse water–gas shift contributing to the high consumption of CO_2 reactant.

Effect of operating conditions

Apart from catalyst property, the process variables such as volume hourly space velocity (VHSV), reaction temperature and reactant partial pressure also play essential role to formulate the inherent kinetic models for catalyst based on elementary steps since the reaction kinetics are fundamentally affected by resistances of mass and heat transfer associated with process variables (Abdullah et al. 2017). Hence, wide-ranging investigations of process variable on microwave-assisted DRM were conducted to describe the correlation between operating conditions and the corresponding catalytic performance meanwhile determine the appropriate optimization of microwave-assisted DRM process conditions (Fidalgo et al. 2008; Gangurde et al. 2018; Odedairo et al. 2016). Catalytic performance of catalysts under varying process variables reported in literature is listed in Table 6.

Reaction temperature

The increase in reaction temperature profoundly offers positive effects to the microwave-assisted DRM since the reaction is intrinsically possessing endothermic nature. However, analogous to other reforming processes, catalyst deactivation caused by metal sinterization and carbon deposits was the unavoidable encountered setback at extreme temperature condition. Thus, numerous researches were to determine the appropriate temperature range for performing microwave-assisted DRM in terms of excellent reforming performance and insignificant carbonaceous deposition.

Fidalgo et al. (2008) examined the temperature impact on microwave-assisted DRM performance over activated carbon at reaction temperature of 600–900 °C. They found that the temperature range 700–800 °C was appropriate for maximizing the reforming performance due to the existence of microplasmas facilitating the heterogeneous catalytic reactions, namely, CH_4 dissociation and CO_2 gasification. However, higher temperatures accelerated the growth of carbonaceous species encapsulating active sites of catalyst while lower temperatures only achieved low CH_4 conversion (36%) and CO_2 conversion (25%). Similarly, Domínguez et al. (2007a, b) found that increasing reforming temperature could generate microplasmas during microwave heating approach which appreciably improved the CH_4 conversion of activated carbon from 11 to 70% at VSHV of 160 ml g_{cat}^{-1} h^{-1} (Domínguez et al. 2007a, b). However, the reactant conversions declined with reaction duration owing to the pore blockage of catalyst induced by carbon deposition, as evidenced by the reduction in micropore volumes and BET surface area. Additionally, Lim and Chun (2017) and Zhang et al. (2018b) stated that growth in reactant conversions with increasing temperature was mainly ascribed to the endothermicity of microwave-assisted DRM (Lim and Chun 2017; Zhang et al. 2018b). From the study, Zhang et al. (2018b) discovered that as temperature increased, CH_4 conversion was lower than CO_2 conversion under microwave irradiation, indicating the predominance of reverse Boudouard reaction and water–gas shift reaction.

From the investigation of transition metal-promoted, i.e. Ta, Cr and Fe, Ni catalysts for microwave-assisted DRM with different microwave heating powers, Odedairo et al. (2016) concluded that a growth in temperature from 770 to 940 °C could greatly influence the coke formation and improve the catalytic activity. However, this behaviour was enormously depending on the ability of microwave absorption for material employed and the carbonaceous species formed on catalyst surface. Odedairo et al. (2016) assigned the superior catalytic performance of 2%Cr–40%Ni/CeO_2 and 2%Ta–40%Ni/CeO_2 to the formation of graphene at suitable reaction temperatures associated with the microwave heating power. The subsequent in situ graphene could further enhance the heat dissipation from microwave and locally heated the neighbouring Ni particles and thus improvement of catalytic activity. Hamzehlouia et al. (2018) synthesized a carbon-coated SiO_2 catalyst and examined at varying operating temperatures from 650 to 900 °C (Hamzehlouia et al. 2018). The reactant conversions were in accordance with the microwave-assisted DRM endothermic nature, in which CO_2 and CH_4 conversions were improved up to 85% and 91%, correspondingly by increasing the reaction temperature (Fig. 19). With the employment of microwave heating, the reactant conversions achieved were reportedly greater than thermodynamically predicted equilibrium values reported in literature. Hence, Hamzehlouia et al. (2018) proposed that the microwave selective heating mechanism not only enhanced the reforming performance via sustainably maintain the temperature gradient on catalyst surface

Table 6 Effects of process variables on the catalytic performance for microwave-assisted dry reforming of methane (DRM) reaction with different catalysts

Catalysts and microwave receptors (C/MR)	Operating conditions			CH_4 conversion (%)	CO_2 conversion (%)	H_2/CO ratio	References
	CH_4/CO_2 ratio	Temperature (°C)	VHSV (Ml g_{cat}^{-1} h^{-1})				
Activated carbon (filtracarb FY5)	1/1.5	600–800	400	36–100	25–100	0.90–0.70	Fidalgo et al. (2008)
	0.4–0.65/0.6–0.35	800	160	100–31	100–65	0.70–1.40	
	1/1	800	320–920	70–38	80–44	0.80–0.70	
Activated carbon (filtracarb FY5)	–	700–900	160	11–70	–	–	Domínguez et al. (2007a, b)
	–	800	160–720	80–20	–	–	
Sludge char[a]	1/1	800–1000	300	61–76	74–88	1.03–1.58	Lim and Chun (2017)
	1/1	900	300–1300	72–35	77–35	1.24–1.42	
C-SiO_2	1/1	650–900	–	76–91	57–85	–	Hamzehlouia et al. (2018)
8%Pt/20%CeO_2/γ-Al_2O_3	1/1	450–800	7200	29–92	38–91	0.53–0.96	Zhang et al. (2003)
	3–1/1–3	650	7200	36–89	95–48	1.19–0.53	
Ni/CeO_2	1/1	770–940	10,200	45–78	–	–	Odedairo et al. (2016)
2%Ta–40%Ni/CeO_2	1/1	770–940	10,200	55–81	–	–	Odedairo et al. (2016)
2%Fe–40%Ni/CeO_2	1/1	770–940	10,200	48–69	–	–	Odedairo et al. (2016)
2%Cr–40%Ni/CeO_2	1/1	770–940	10,200	82–90	–	–	Odedairo et al. (2016)
12%Fe/Al_2O_3–SiC	1/1	427–773	200[b]	0–95	0–97	–	Zhang et al. (2018b)
	1/1	750	200–800[b]	96–80	94–82	1.23–1.07	
7%Ru/$SrTiO_3$	1/1	415–1068	3000	12–81	16–78	0.60–0.86	Gangurde et al. (2018)
	0.55–0.4/0.45–0.6	1068	3000	69–94	95–85	0.97–0.81	
	0.45/0.55	≥ 1068	3000–13,500	90–54	89–65	0.88–0.86	
10%Fe–C	2–0.5/1	800	7200	84–99	95–99	1.72–0.48	(Li et al. 2019)

[a]Sludge char was composed of SiO_2 (28.35 wt%), P_2O_5 (24.76 wt%), Al_2O_3 (13.09 wt%), CaO (12.06 wt%), Fe_2O_3 (8.98 wt%), MgO (4.55 wt%), K_2O (2.64 wt%), SO_3 (2.05 wt%), ZnO (0.56 wt%), CuO (0.35 wt%), BaO (0.20 wt%), MnO (0.16 wt%), SrO (0.07 wt%) and NiO (0.04 wt%)

[b]The volume hourly space velocity (VHSV) unit was h^{-1}

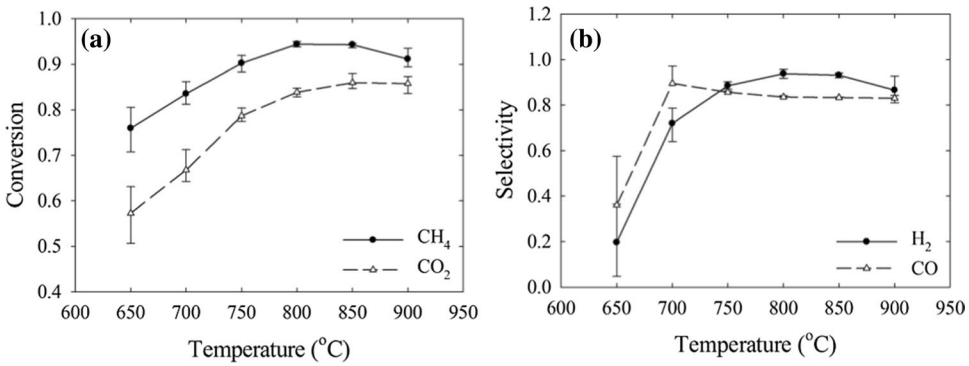

Fig. 19 **a** Reactant conversion and **b** product selectivity at temperature ranging from 650 to 900 °C. The reactant conversion and product selectivities are enormously enhanced with the employment of microwave heating compared to conventional electric heating method. This indicates that microwave selective heating mechanism not only improves the reforming performance by retaining the temperature gradient on catalyst surface but also greatly hinders the occurrence of secondary gas-phase reactions. Adapted from Hamzehlouia et al. (2018)

but also highly inhibited the occurrence of secondary gas-phase reactions to achieve the remarkable H_2 and CO selectivities (Fig. 19).

Gas hourly space velocity

Apart from the reaction temperature, mass transport of reactants also play a substantial role to the derivation of kinetic models associated with elementary steps. The conversions of reactant can be straightforwardly ascribed to the fundamental kinetics of the catalysts if the mass transport resistance is negligible (Abdullah et al. 2017). Hence, in order to diminish mass transport resistance, evaluation of volume hourly space velocity is necessary for determining the independence of reactant conversions to volume hourly space velocity after reaching a steady-state (Kathiraser et al. 2015).

Domínguez et al. (2007a, b) scrutinized the volume hourly space velocity effect on the catalyst behaviour for microwave-assisted DRM by using FY5 at 800 °C with 120 min and revealed that growing VSHV from 160 to 720 ml g_{cat}^{-1} h^{-1} resulted in a decline in CH_4 conversion from 80 to 20%. This observation was ascribed to the short contact time between methane gaseous reactant and active sites on activated carbon surface during the microwave-assisted DRM (Domínguez et al. 2007a, b). Moreover, Fidalgo et al. (2008) described analogous findings of the negative effect of increasing volume hourly space velocity on CH_4 conversion over sludge char catalysts owing to the reduced retention time for heterogeneous catalytic reaction. They suggested that longer retention time favoured the carbon gasification by CO_2 and CH_4 decomposition, leading to a decrease in reactant conversions while H_2/CO ratio was retained (Fidalgo et al. 2008). In the study of influential factors for microwave-assisted DRM over Fe catalysts, Zhang et al. (2018b) also found that a rise in VSHV ranging of 200–800 h^{-1} resulted in the CH_4 and CO_2 conversion declined by 15.2% and 13.1% in this order. This observation was ascribed to the drop in the reactants' retention time on the surface of catalyst with rising VSHV (Zhang et al. 2018b). Nevertheless, they reported that H_2/CO of syngas generated was not significantly affected with rising volume hourly space velocity in line with the findings obtained by Fidalgo et al. (2008) and Gangurde et al. (2018).

Reactant partial pressure

The microwave-assisted DRM reaction is an endothermic reforming process which is capable to generate syngas with fraction of H_2 to CO less than unity at temperature range of 700–1100 °C under microwave irradiation. In fact, ratio of H_2/CO less than 1 is a valuable feedstock favoured for downstream Fischer–Tropsch (FT) synthesis and methanol production (Abdullah et al. 2017; Siang et al. 2018). Thus, evaluation of various reactant feed composition effect on microwave-assisted DRM is exceptionally important for tuning appropriate H_2/CO ratios with respect to industrial necessity.

Zhang et al. (2003) inspected the impact of feed composition on the conversions and product selectivities at 650 °C with CO_2/CH_4 ratios ranging of 1:3–3:1 for both microwave heating and conventional approaches. They noticed that growing CO_2/CH_4 ratio resulted in a rise in CH_4 conversion but reduced the CO_2 conversion. A comparable conversion value of CH_4 and CO_2 was attained at CO_2/CH_4 ratio around 1.2 due to the evolution of secondary reaction associated with CO_2 at CO_2-rich environment. However, H_2/CO ratio was declined from 1.19 to 0.53 with rising CO_2 reactant implying that reverse water–gas shift was dominant. In the study of microwave-assisted DRM, Fidalgo et al. (2008) stated that influence of CO_2 partial pressure in feed gas on reforming performance was significant than that of reaction temperature. Similar to results attained by Zhang et al. (2003), the reactant conversions increased with growing CO_2/CH_4 ratio. Additionally, a drop in reactant conversions was obtained at low CO_2 concentration, possibly due to the deficiency of regenerated catalyst active sites of via carbon gasification by CO_2 (Zhang et al. 2003). Gangurde et al. (2018) also reported analogous findings and proposed that an increase in CO_2 gaseous reactant in feed gas could lead to an acceleration in deposited carbon gasification and thus facilitating the regeneration of active sites and improving the reactant conversions (Gangurde et al. 2018).

Li et al. (2019) have conducted microwave-assisted DRM over Fe-rich biomass-derived char under different feedstock ratios to determine the correlation between the feed composition and Fe content presented on catalysts. As CH_4/CO_2 ratio increased, an observed decline in catalytic activity implying the predominance of carbon deposition originated from CH_4 decomposition at CH_4-rich environment. Notably, the CO_2 conversion obtained was stable and was higher than CH_4 conversion regardless the reactant partial pressure. This observation reveals that the rates of both gasification of carbonaceous deposits and reverse water–gas shift were accelerated with the presenting Fe content in char compared to original char. This evolution could explain the decline in H_2/CO ratio (from 1.72 to 0.48) at lower ratio of CH_4 to CO_2 due to the excessive CO gas produced from the parallel side reactions.

As partial conclusions, the employment of natural gas in chemical and energy industries has driven exceptional impacts on the world in terms of economic and environmental outlooks. However, the development of efficient approach to sustainably convert natural gas to value-added syngas product with low capital cost is always a challenging topic. The microwave-assisted DRM offers environmental advantages since it consumes anthropogenic CO_2 greenhouse gas

leading to a reduction in global CO_2 emission. In addition, by utilizing the intrinsic dielectric property of material with microwave interaction, strong thermal gradients could be generated between the gaseous reactants and catalyst with the existence of microwave irradiation promoting the syngas selectivity and concurrently retaining the reactant conversions and eliminating the occurrence of secondary gas-phase reactions.

Nevertheless, catalyst deactivation induced by carbonaceous deposition is one of major drawbacks to reforming technologies for industrial implementation. microwave-assisted DRM over carbon-containing catalysts, combining catalytic and dielectric attributes with microwave irradiation to substantially improve the rate of catalytic heterogeneous reaction and reforming performance. Hence, future study in this realm is possibly to highlight on the exploration of appropriate materials combined as catalyst and microwave receptors possessing high surface areas to accommodate the catalyst active sites.

Numerous studies on microwave-assisted DRM showed very promising catalytic performance owing to its selective mechanism with existing microwave heating. Additionally, the influence of microwave heating on thermodynamic equilibrium, activation energy and kinetic parameters exhibits valuable information to understand the reaction mechanistics and formation of intermediate compounds. Substantial evolutions have been evidenced in the last years but further studies are still necessitated in future works in order to develop the best-fitted kinetic modelling fundamentally derived from mechanistic reaction pathways.

Energy consumption comparison

The capability of the microwave energy for non-contact, rapid, and selective heating promoted its application in distinct research disciplines across the globe in the last couple of decades (Bermudez et al. 2015). As comprehensively validated in previous sections of this review, it has been extensively applied in dry reforming of methane too. However, comparative assessment on energy consumption of conventional and microwave heating in the dry reforming of methane is seldom done. The total publications with and without energy efficiency conclusion during the last decades is summarized in Fig. 20 (Scopus® data were used). It depicts that despite the increasing interest in dry reforming of methane technology for industrialization, minimal research works dedicated to energy efficiency have been performed, in precise less than 1% amongst around 2300 research works considered for this comparison. The energy efficiency of the conventional furnace is even less ominously studied compared to those with plasma or microwave-assisted heating, yet they are inconclusive.

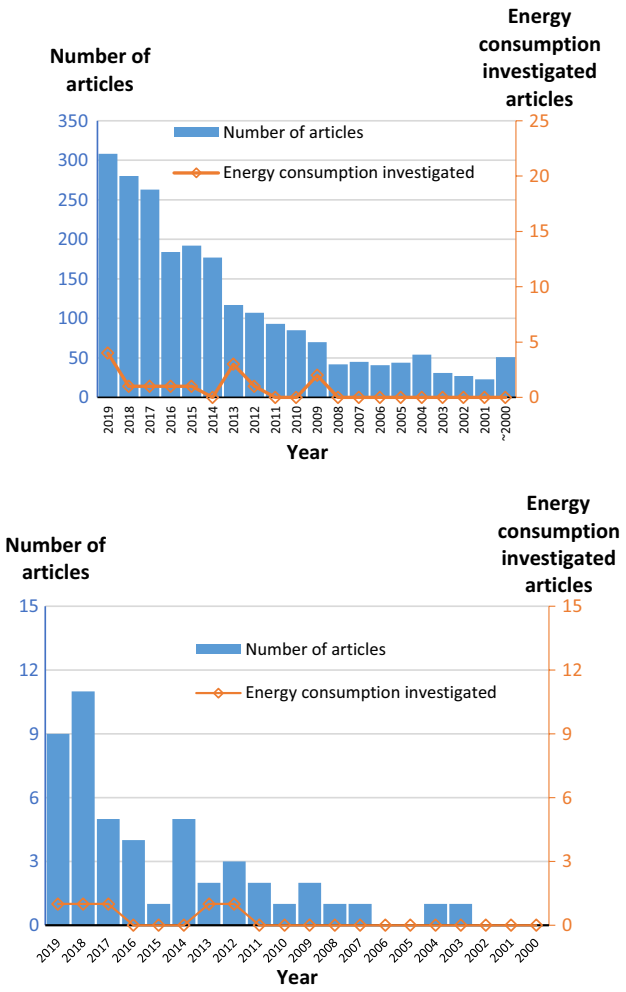

Fig. 20 Publication distribution in the history of the dry reforming of methane to produce syngas. Top: methane reforming with and without energy consumption conclusion; bottom: microwave-assisted methane reforming with and without energy consumption conclusion. It is evident that minimal research works dedicated to energy efficiency studies. (*Source*: Scopus®)

It is evidently confirmed that microwave heating excelled in CH_4–CO_2 conversion performance compared to conventional furnace heating in terms of energy consumption and heating rates (Fidalgo et al. 2008; Gangurde et al. 2018). Hence, the microwave energy directly transfers to the microwave receptor/catalysts and enhances the internal temperature with precisely uniform distribution, eluding the energy wastage by heating the environs and reactor wall. However, a comprehensive comparison study between conventional and microwave heating is yet to be done. Fidalgo and Menéndez (2012) inspected the energy consumption in a microwave pilot plant and scaled up the results to compare energy efficiency with industrially established processes. They estimated that 50% FY5 + 50% Ni/Al_2O_3 catalyst consumed 4.6 kW h/m^3 of H_2 produced; FY5 means coconut

shell-derived activated carbon. Tian et al. (2019) reported that the energy consumption for CO_2 utilization in a conventional furnace reactor is 682 kJ/mol. Table 7 compares the energy consumption in the dry reforming of methane with different heating sources. A comparison within the bibliographic data is almost impossible as their experimental conditions are far different.

Scaling up of dry reforming process is inevitable in the coming years. Hence, the relevance of microwave-assisted dry reforming of methane in the large scale over conventional methods is yet to prove on a case-to-case basis, considering equipment design, radiation frequency, mode of heating, specific power, energy balance, and energy losses through the reactor wall (Bermudez et al. 2015). It could be suggested to start with simulation studies using basic tools such as ASPEN in order to compare mass and energy balance of the conventional dry reforming of methane and microwave-assisted DRM. PINCH analysis could be also used to optimize and compare energy consumption of these reforming processes. Microwave heating exhibits exclusive advantages over conventional heating. However, it is worth to consider that the energy saving in microwave-assisted catalytic synthesis reactions are connected to the shortened reaction time, not any of the microwave features (Razzaq and Kappe 2008). Hence, such shortening of reaction time in the reforming experiments has many challenges. It demands to develop suitable catalysts capable of reforming feed gases at high flow rates too. All the while, the energy consumption in the microwave-assisted reforming is reliant on the efficiency of microwave susceptor (Razzaq and Kappe 2008). So, the development of efficient susceptor capable of stable feed conversion at high flow would be a breakthrough in the industrialization of microwave reforming.

Conclusion

As an alternative to the steam reforming of methane which is a well-established industrial process for syngas production, the dry reforming of methane has shown various environmental benefits since it converts greenhouse gases, especially non-combustible CO_2, into syngas as high-value platform chemicals. However, in order to be more competitive, the dry reforming of methane system must be improved both in terms of energy consumption and catalytic performance. Being assisted by microwave heating, which exhibits exclusive advantages over conventional one, the dry reforming of methane has given rise to promising results, thus deserved to be investigated deeply. There are several potential avenues to explore further microwave-assisted DRM; thus, the following outlooks are pointed out:

Table 7 A comparison on energy consumption in methane dry reforming with various heating sources

Catalyst/MW susceptor	Heating source	Feed flow	H_2:CO ratio	Supplied power	Energy consumption	References
FY5	Microwave	0.72 kg/h[a]	2:3	84.4 kW	44.4 kW h/m^3[b]	Fidalgo and Menéndez (2012)
FY5 + Ni/Al_2O_3	Microwave	0.72 kg/h	1:1	8.3 kW	4.6 kW h/m^3[b]	Fidalgo and Menéndez (2012)
Bio-char	Microwave	1 m^3/h[a]	1:1.1	13.2 kW	4.14 kW h/m^3[c]	Li et al. (2018a, b)
HyProGen R-70	Microwave	30 L/min	0.25:1.5	3 kW	59.1 g/kWh[b]	Chun et al. (2019)
Ni/bio-char	Microwave	1.2 L/h/g	1:1.5	12.8 kW/kg	7.9 kW/hm^3[c]	Li et al. (2017)
–	Microwave plasma torch		1:1	6 kW	41.4 g/kWh[b]	Chun et al. (2017)
–	Gliding arc discharge plasma	12.7 SL/min	1:1	5.91 kV	3.2 eV	Bo et al. (2008)
CaO–Ni (looping)	Electric furnace	–	1:0.9	–	534.8 kJ/mol	Tian et al. (2019)
CaO–Ni	Electric furnace	–	1:1	–	682 kJ/mol[d]	Tian et al. (2019)
–	Plasma	50 mL/min	–	30 W	0.14 mmol/kJ	Tu and Whitehead (2012)
Ni/-Al_2O_3	Plasma	50 mL/min	–	30 W	0.32 mmol/kJ	Tu and Whitehead (2012)
–	DBD	200 mL/min	–	50 W	5.47 g/kWh[b]	Dors et al. (2012)

[a]With respect to CH_4 conversion

[b]With respect to produced H_2

[c]With respect to produced syn-gas

[d]With respect to CO_2 conversion

(1) The existence of microplasmas was found to be responsible for facilitating some preferred catalytic reactions, such as CH_4 dissociation and CO_2 gasification. Although it is well-established that the main reactions of the dry reforming of methane are favourable at high temperature, low pressure and a low molar ratio of CH_4/CO_2, there is a need to develop the thermodynamic equilibrium models which take into account the formation of hotspots or microplasmas to provide improved estimates of overall efficiencies.

(2) Many studies on the microwave-assisted DRM have been focused on the carbon-based catalysts due to their reasonable catalytic and dielectric properties. However, the formation of coke which causes severe blockage of active sites and disappearance of carbonaceous catalytic materials due to the CO_2 gasification reaction seems to be unavoidable during the reforming process. Thus, there remains scope to further increase the performance and stability of carbon-based catalysts by altering the operational conditions so that carbon produced will be consumed immediately.

(3) Due to its high magnetic loss tangent and well-established catalytic properties towards the dry reforming of methane, Ni-based catalysts deserve to be studied more thoroughly. Although metal is classified as a microwave reflector, it can be effectively heated by microwave as long as its particle is fine enough compared to its penetration depths. Since most of microwave susceptors have low surface area whereas porous supports are transparent, it also worth noting that a transparent material will become more lossy to be able to absorb microwaves at a higher temperature. Therefore, there is some potential to maximize the performance of Ni-based catalysts on microwave-assisted DRM: (1) increasing the amount of fine (nano-size) Ni particles coated on the micro- or mesoporous materials, which have been widely employed as the effective supports for the conventional dry reforming of methane, as much as possible to improve their microwave absorbing ability; (2) mixing any effective Ni-based catalyst with high lossy materials such as SiC; and (3) combining these two approaches to form a two-way heating: conventional heating from the surface by susceptor-generated thermal radiation and microwave heating from the centre, resulting in more uniform heating.

(4) Any material that can act efficiently as both catalyst for the conventional dry reforming of methane and microwave susceptor may exhibit excellent activity for microwave-assisted DRM. High lossy materials such as metal carbides, perovskites and ferrites, which have been proved to have outstanding catalytic activity and stability for the dry reforming of methane, deserve to be employed in microwave-assisted DRM according to this approach.

(5) The prospect of actual application of an alternative technology depends on many factors that are inherently related to the equipment design and process optimization, such as the energy efficiency, the potential scalability, and the benefits of the alternative technology compared to the conventional one. The development of microwave equipment for different heating purposes is in progress, ranging from the commercial to the conceptual stage. Drawing from this related area may lead to an approach for improving the design and scale-up of a microwave-assisted reforming system.

(6) Further simulation and experimental works need to be done to optimize and compare energy consumption as well as the overall efficiency of the conventional and microwave-assisted reforming processes. It could be suggested to start with simulation studies using basic tools such as ASPEN in order to compare mass and energy balance of the conventional dry reforming of methane and microwave-assisted DRM. PINCH analysis could be also used to optimize and compare the energy consumption of these reforming processes. Comparison should be experimentally validated on a case-to-case basis, keeping the same operating conditions such as, reactor design, catalysts used, reaction temperature, gas hourly space velocity, and reactant composition.

Acknowledgements A part of this work is funded by Vietnam National Foundation for Science and Technology Development (NAFOSTED) under Grant Number "104.05-2019.344" for the project entitled "Syngas generation from bi-reforming of biomass-derived feedstocks using microwave-enhanced reactor". A part of this work was financially supported by The Japan Society for the Promotion of Science (JSPS) for Grant-Aid for Challenging Research (Pioneering) (17H06225). The authors are also grateful to the Cooperative Research Program of Network Joint Research Center for Materials and Devices that has been supported by Ministry of Education, Culture, Sports, Science, and Technology (MEXT), Japan.

References

Abdullah B, Abd Ghani NA, Vo DVN (2017) Recent advances in dry reforming of methane over Ni-based catalysts. J Clean Prod 162:170–185. https://doi.org/10.1016/j.jclepro.2017.05.176

Abdulrasheed A, Jalil AA, Gambo Y, Ibrahima M, Hambali HU, Hamid HYS (2019) A review on catalyst development for dry reforming of methane to syngas: recent advances. Renew Sustain Energy Rev 108:175–193. https://doi.org/10.1016/j.rser.2019.03.054

Alia S, Khader MM, Almarri MJ, Abdelmoneim AG (2020) Ni-based nano-catalysts for the dry reforming of methane. Catal Today 343:26–37. https://doi.org/10.1016/j.cattod.2019.04.066

Antunes E, Jacob MV, Brodie G, Schneider PA (2018) Microwave pyrolysis of sewage biosolids: dielectric properties, microwave

susceptor role and its impact on biochar properties. J Anal Appl Pyrol 129:93–100. https://doi.org/10.1016/j.jaap.2017.11.023
Aramouni NAK, Touma JG, Tarboush BA, Zeaiter J, Ahmad MN (2018) Catalyst design for dry reforming of methane: analysis review. Renew Sustain Energy Rev 82:2570–2585. https://doi.org/10.1016/j.rser.2017.09.076
Aravind S, Kumar PS, Kumar NS, Siddarth N (2020) Conversion of green algal biomass into bioenergy by pyrolysis. A review. Environ Chem Lett 18:829–849. https://doi.org/10.1007/s10311-020-00990-2
Arora S, Prasad R (2016) An overview on dry reforming of methane: strategies to reduce carbonaceous deactivation of catalysts. RSC Adv 6:108668–108688. https://doi.org/10.1039/C6RA20450C
Atwater J, Wheeler R (2004) Temperature dependent complex permittivities of graphitized carbon blacks at microwave frequencies between 0.2 and 26 GHz. J Mater Sci 39:151–157. https://doi.org/10.1023/B:JMSC.0000007739.07797.08
Balajii M, Niju S (2019) Biochar-derived heterogeneous catalysts for biodiesel production. Environ Chem Lett 17:1–23. https://doi.org/10.1007/s10311-019-00885-x
Barbosa-Canovas GV, Ibarz A (2014) Introduction to food process engineering. CRC Press, Boca Raton
Benedito A, Galindo B, Hare C, Morgan L, Bayerl T, Mitschang P (2012) Selective heating applications for the processing of polymer–polymer materials. In: Proceedings of the 15th European conference on composite materials (ECCM-15), Venice, Italy
Beneroso D, Fidalgo B (2016) Microwave technology for syngas production from renewable sources. In: Myers R (ed) Syngas: production, emerging technologies and ecological impacts. Nova Science Publishers, Hauppauge, NY (USA), pp 117–152
Benrabaa R, Löfberg A, Rubbens A, Bordes-Richard E, Vannier RN, Barama A (2013) Structure, reactivity and catalytic properties of nanoparticles of nickel ferrite in the dry reforming of methane. Catal Today 203:188–195. https://doi.org/10.1016/j.cattod.2012.06.002
Bermudez JM, Fidalgo B, Arenillas A, Menéndez JA (2012) Mixtures of steel-making slag and carbons as catalyst for microwave-assisted dry reforming of CH_4. Chin J Catal 33:1115–1118. https://doi.org/10.1016/S1872-2067(11)60386-0
Bermudez JM, Beneroso D, Rey-Raap N, Arenillas A, Menéndez JA (2015) Energy consumption estimation in the scaling-up of microwave heating processes. Chem Eng Process Process Intensif 95:1–8. https://doi.org/10.1016/j.cep.2015.05.001
Bhaskar A, Chang TH, Chang HY, Cheng SY (2007) Low-temperature crystallization of sol–gel-derived lead zirconate titanate thin films using 2.45 GHz microwaves. Thin Solid Films 515:2891–2896. https://doi.org/10.1016/j.tsf.2006.08.044
Bhattacharya M, Basak T (2016) A review on the susceptor assisted microwave processing of materials. Energy 97:306–338. https://doi.org/10.1016/j.energy.2015.11.034
Bo Z, Yan J, Li X, Chi Y, Cen K (2008) Plasma assisted dry methane reforming using gliding arc gas discharge: effect of feed gases proportion. Int J Hydrog Energy 33:5545–5553. https://doi.org/10.1016/j.ijhydene.2008.05.101
BP Statistical Review of World Energy (2019) 68th edition. https://www.bp.com/en/global/corporate/energy-economics/statistical-review-of-world-energy.html. Accessed 15 June 2020
Cao Z, Yoshikawa N, Taniguchi S (2010) Microwave heating behaviors of Si substrate materials in a single-mode cavity. Mater Chem Phys 124:900–903. https://doi.org/10.1016/j.matchemphys.2010.08.004
Chein RY, Chen YC, Yu CT, Chung JN (2015) Thermodynamic analysis of dry reforming of CH_4 with CO_2 at high pressures. J Nat Gas Chem 26:617–629. https://doi.org/10.1016/j.jngse.2015.07.001
Chen MQ, Wang J, Zhang MX, Chen MG, Zhu XF, Min FF, Tan ZC (2008) Catalytic effects of eight inorganic additives on pyrolysis of pine wood sawdust by microwave heating. J Anal Appl Pyrol 82:145–150. https://doi.org/10.1016/j.jaap.2008.03.001
Chen W, Sheng W, Cao F, Lu Y (2012) Microfibrous entrapment of Ni/Al_2O_3 for dry reforming of methane: heat/mass transfer enhancement towards carbon resistance and conversion promotion. Int J Hydrog Energy 37(23):18021–18030. https://doi.org/10.1016/j.ijhydene.2012.09.080
Cheng J, Roy R, Agrawal D (2001) Experimental proof of major role of magnetic field losses in microwave heating of metal and metallic composites. J Mater Sci Lett 20:1561–1563. https://doi.org/10.1023/A:1017900214477
Cheng J, Roy R, Agrawal D (2002) Radically different effects on materials by separated microwave electric and magnetic fields. Mater Res Innov 5:170–177. https://doi.org/10.1007/s10019-002-8642-6
Chun SM, Hong YC, Choi DH (2017) Reforming of methane to syn-gas in a microwave plasma torch at atmospheric pressure. J CO2 Util 19:221–229. https://doi.org/10.1016/j.jcou.2017.03.016
Chun SM, Shin DH, Ma SH, Yang GW, Hong YC (2019) CO_2 Microwave plasma-catalytic reactor for efficient reforming of methane to syngas. Catalysts 9(3):292. https://doi.org/10.3390/catal9030292
De Caprariis B, De Filippis P, Petrullo A, Scarsella M (2015) Methane dry reforming over nickel perovsikite catalysts. Chem Eng Trans 43:991–996. https://doi.org/10.3303/CET1543166
Domínguez A, Fernández Y, Fidalgo B, Pis JJ, Menéndez JA (2007a) Biogas to syngas by microwave-assisted dry reforming in the presence of char. Energy Fuels 21:2066–2071. https://doi.org/10.1021/ef070101j
Domínguez A, Fidalgo B, Fernández Y, Pis JJ, Menéndez JA (2007b) Microwave-assisted catalytic decomposition of methane over activated carbon for CO_2-free hydrogen production. Int J Hydrog Energy 32:4792–4799. https://doi.org/10.1016/j.ijhydene.2007.07.041
Dors M, Izdebski T, Berendt A, Mizeraczyk J (2012) Hydrogen production via biomethane reforming in DBD reactor. Int J Plasma Environ Sci Technol 6:93–97. https://doi.org/10.34343/ijpest.2012.06.02.093
Durka T, Van Gerven T, Stankiewicz A (2009) Microwaves in heterogeneous gas-phase catalysis: experimental and numerical approaches. Chem Eng Technol 32:1301–1312. https://doi.org/10.1002/ceat.200900207
Durka T, Stefanidis GD, Van Gerven T, Stankiewicz AI (2011) Microwave-activated methanol steam reforming for hydrogen production. Int J Hydrog Energy 36:12843–12852. https://doi.org/10.1016/j.ijhydene.2011.07.009
Ellison C, McKeown M, Trabelsi S, Boldor D (2017) Dielectric properties of biomass/biochar mixtures at microwave frequencies. Energies 10:502. https://doi.org/10.3390/en10040502
Eskilsson CS, Björklund E (2000) Analytical-scale microwave-assisted extraction. J Chromatogr A 902(1):227–250. https://doi.org/10.1016/S0021-9673(00)00921-3
Estel L, Poux M, Benamara N, Polaert I (2017) Continuous flow-microwave reactor: Where are we? Chem Eng Proc Proc Intensif 113:56–64. https://doi.org/10.1016/j.cep.2016.09.022
Fidalgo B, Menéndez JA (2012) Study of energy consumption in a laboratory pilot plant for the microwave-assisted CO_2 reforming of CH_4. Fuel Proc Technol 95:55–61. https://doi.org/10.1016/j.fuproc.2011.11.012
Fidalgo B, Menéndez JA (2013) Syngas production by CO_2 reforming of CH_4 under microwave heating–challenges and opportunities. In: Indarto A, Palguandi J (eds) Syngas: production, applications and environmental impact. Nova Science Publisher, New York, pp 121–149
Fidalgo B, Domínguez A, Pis J, Menéndez JA (2008) Microwave-assisted dry reforming of methane. Int J Hydrog

Energy 33(16):4337–4344. https://doi.org/10.1016/j.ijhydene.2008.05.056
Fidalgo B, Arenillas A, Menéndez JA (2010) Influence of porosity and surface groups on the catalytic activity of carbon materials for the microwave-assisted CO_2 reforming of CH_4. Fuel 89:4002–4007. https://doi.org/10.1016/j.fuel.2010.06.015
Fidalgo B, Arenillas A, Menéndez JA (2011) Mixtures of carbon and Ni/Al_2O_3 as catalysts for the microwave-assisted CO_2 reforming of CH_4. Fuel Proc Technol 92:1531–1536. https://doi.org/10.1016/j.fuproc.2011.03.015
Fischer VF, Tropsch H (1928) Conversion of methane into hydrogen and carbon monoxide. Brennstoff-Chemie 3(9):39–46
Gabriel C, Gabriel S, Grant EH, Grant EH, Halstead BSI, Mingos DMP (1998) Dielectric parameters relevant to microwave dielectric heating. Chem Soc Rev 27:213–224. https://doi.org/10.1039/A827213Z
Gangurde LS, Sturm GS, Devadiga TJ, Stankiewicz AI, Stefanidis AD (2017) Complexity and challenges in noncontact high temperature measurements in microwave-assisted catalytic reactors. Ind Eng Chem Res 56:13379–13391. https://doi.org/10.1021/acs.iecr.7b02091
Gangurde LS, Sturm GSJ, Valero-Romero MJ, Mallada R, Santamaria J, Stankiewicz AI, Stefanidisad GD (2018) Synthesis, characterization, and application of ruthenium-doped $SrTiO_3$ perovskite catalysts for microwave-assisted methane dry reforming. Chem Eng Proc Proc Intensif 127:178–190. https://doi.org/10.1016/j.cep.2018.03.024
Giguere RJ, Bray TL, Duncan SM, Majetich G (1986) Application of commercial microwave ovens to organic synthesis. Tetrahedron Lett 27(41):4945–4948. https://doi.org/10.1016/S0040-4039(00)85103-5
Grouset D, Ridart C (2018) Lowering energy spending and costs for hydrogen transportation and distribution. In: Azzaro-Pantel C (ed) Hydrogen supply chain: design, deployment and operation, 1st edn. Elsevier, Academic Press, pp 207–270. https://doi.org/10.1016/B978-0-12-811197-0.00006-3
Guler M, Dogu T, Varisli D (2017) Hydrogen production over molybdenum loaded mesoporous carbon catalysts in microwave heated reactor system. Appl Catal B Environ 219:173–182. https://doi.org/10.1016/j.apcatb.2017.07.043
Gündüz S, Dogu T (2015) Hydrogen by steam reforming of ethanol over Co–Mg incorporated novel mesoporous alumina catalysts in tubular and microwave reactors. Appl Catal B Environ 168–169:497–508. https://doi.org/10.1016/j.apcatb.2015.01.006
Gupta M, Leong EWW (2008) Microwaves and metals. Wiley, Hoboken
Hamzehlouia S, Jaffer SA, Chaouki J (2018) Microwave heating-assisted catalytic dry reforming of methane to syngas. Sci Rep 8:8940. https://doi.org/10.1038/s41598-018-27381-6
Haneishi N, Tsubaki S, Maitani MM, Suzuki E, Fujii S, Wada Y (2017) Electromagnetic and heat-transfer simulation of the catalytic dehydrogenation of ethylbenzene under microwave irradiation. Ind Eng Chem Res 56:7685–7692. https://doi.org/10.1021/acs.iecr.7b01413
Haque KE (1999) Microwave energy for mineral treatment processes-a brief review. Int J Miner Proc 57:1–24. https://doi.org/10.1016/S0301-7516(99)00009-5
Hashisho Z, Rood MJ, Barot S, Bernhard J (2009) Role of functional groups on the microwave attenuation and electric resistivity of activated carbon fiber cloth. Carbon 47:1814–1823. https://doi.org/10.1016/j.carbon.2009.03.006
Hassan NS, Jalil AA, Hitam CNC, Vo DVN, Nabgan W (2020) Biofuels and renewable chemicals production by catalytic pyrolysis of cellulose: a review. Environ Chem Lett. https://doi.org/10.1007/s10311-020-01040-7
Hawangchu Y, Atong D, Sricharoenchaikul V (2010) Enhanced microwave induced thermochemical conversion of waste glycerol for syngas production. Int J Chem React Eng. https://doi.org/10.2202/1542-6580.2187
Herminio T, Cesário MR, Silva VD, Simões TA, Medeiros ES, Macedo DA, Tidahy HL, Gennequin C, Abi-Aad E (2020) CO_2 reforming of methane to produce syngas using anti-sintering carbon-resistant Ni/CeO_2 fibers produced by solution blow spinning. Environ Chem Lett 18:1–9. https://doi.org/10.1007/s10311-020-00968-0
Higman C (2017) GSTC Syngas Database: 2017 Update. In: Gasification & Syngas Technologies Conference, Colorado Springs. https://www.globalsyngas.org/uploads/downloads/keynote%20tuesday%20eve%20Higman.pdf. Accessed 22 July 2020
Hogan PF, Mori T (1990) Development of a method of continuous temperature measurement for microwave denture processing. Dental Mater J 9:1–11. https://doi.org/10.4012/dmj.9.1
Hoogenboom R, Schubert US (2007) Microwave-assisted polymer synthesis: Recent developments in a rapidly expanding field of research. Macromol Rapid Commun 28:368–386. https://doi.org/10.1002/marc.200600749
Horikoshi S, Sumi T, Serpone N (2012) Unusual effect of the magnetic field component of the microwave radiation on aqueous electrolyte solutions. J Microw Power Electromagn Energy 46:215–228. https://doi.org/10.1080/08327823.2012.11689838
Horikoshi S, Schiffmann RF, Fukushima J, Serpone N (2018) Microwave chemical and materials processing. Springer, Berlin
Hotta M, Hayashi M, Lanagan MT, Agrawal DK, Nagata K (2011) Complex permittivity of graphite, carbon black and coal powders in the ranges of X-band frequencies (8.2 to 12.4 GHz) and between 1 and 10 GHz. ISIJ Int 51:1766–1772. https://doi.org/10.2355/isijinternational.51.1766
Jain S, Newman D, Nzihou A, Dekker H, Le Feuvre H, Richter H, Gobe F, Morton C, Thompson R (2019) Global potential of biogas. World Biogas Association, London
Janezic MD, Paulter N, Blendell J (2001) Dielectric and conductor-loss characterization and measurements on electronic packaging materials. NIST technical note, vol 1520
Jang WJ, Jshim JO, Kim HM, Yoo SY, Roh HS (2019) A review on dry reforming of methane in aspect of catalytic properties. Catal Today 324:15–26. https://doi.org/10.1016/j.cattod.2018.07.032
Jones DA, Lelyveld T, Mavrofidis S, Kingman S, Miles N (2002a) Microwave heating applications in environmental engineering-a review. Res Conserv Recycl 34(2):75–90. https://doi.org/10.1016/S0921-3449(01)00088-X
Jones DA, Lelyveld TP, Mavrofidis SD, Kingman SW, Miles NJ (2002b) Microwave heating applications in environmental engineering-a review. Res Conserv Recycl 34:75–90. https://doi.org/10.1016/S0921-3449(01)00088-X
Julian I, Pedersen CM, Achkasov K, Hueso JL, Hellstern HL, Silva H, Mallada R, Davis ZJ, Santamaria J (2019) Overcoming stability problems in microwave-assisted heterogeneous catalytic processes affected by catalyst coking. Catalysts 9:867. https://doi.org/10.3390/catal9100867
Kathiraser Y, Oemar U, Saw ET, Li Z, Kawi S (2015) Kinetic and mechanistic aspects for CO_2 reforming of methane over Ni based catalysts. Chem Eng J 278:62–78. https://doi.org/10.1016/j.cej.2014.11.143
Kingman SM, Jackson K, Bradshaw SM, Rowson NA, Greenwood R (2004) An investigation into the influence of microwave treatment on mineral ore comminution. Powder Technol 146:176–184. https://doi.org/10.1016/j.powtec.2004.08.006
Komarneni S, Roy R, Li QH (1992) Microwave-hydrothermal synthesis of ceramic powders. Mater Res Bull 27:1393–1405. https://doi.org/10.1016/0025-5408(92)90004-J

Lavoie JM (2014) Review on dry reforming of methane, a potentially more environmentally-friendly approach to the increasing natural gas exploitation. Front Chem 2:1–17. https://doi.org/10.3389/fchem.2014.00081

Li Y, Wang Y, Zhang X, Mi Z (2008) Thermodynamic analysis of autothermal steam and CO_2 reforming of methane. Int J Hydrog Energy 33:2507–2514. https://doi.org/10.1016/j.ijhydene.2008.02.051

Li L, Song Z, Li Z, Zhao X, Ma C (2011) Microwave-assisted reforming of CH_4 with CO_2 over activated carbon. In: 2011 Asia-Pacific power and energy engineering conference, pp 1–4

Li L, Jiang X, Wang H, Wang J, Song Z, Zhao X, Ma C (2017) Methane dry and mixed reforming on the mixture of bio-char and nickel-based catalyst with microwave assistance. J Anal Appl Pyrol 125:318–327. https://doi.org/10.1016/j.jaap.2017.03.009

Li L, Chen J, Yan K, Qin X, Feng T, Wang J, Wang F, Song Z (2018a) Methane dry reforming with microwave heating over carbon-based catalyst obtained by agriculture residues pyrolysis. J CO2 Util 28:41–49. https://doi.org/10.1016/j.jcou.2018.09.010

Li L, Yang Z, Chen J, Qin X, Jiang X, Wang F, Song Z, Ma C (2018b) Performance of bio-char and energy analysis on CH_4 combined reforming by CO_2 and H_2O into syngas production with assistance of microwave. Fuel 215:655–664. https://doi.org/10.1016/j.fuel.2017.11.107

Li L, Yan K, Chen J, Feng T, Wang F, Wang J, Song Z, Ma C (2019) Fe-rich biomass derived char for microwave-assisted methane reforming with carbon dioxide. Sci Total Environ 657:1357–1367. https://doi.org/10.1016/j.scitotenv.2018.12.097

Lim MS, Chun YN (2017) Biogas to syngas by microwave-assisted reforming in the presence of char. Energy Fuels 31:13761–13768. https://doi.org/10.1021/ef070101j

Liu K, Song C, Subramani V (2009) Hydrogen and syngas production and purification technologies. Wiley, Hoboken

Liu S, Zhang Y, Tuo K, Wang L, Chen G (2018) Structure, electrical conductivity, and dielectric properties of semi-coke derived from microwave-pyrolyzed low-rank coal. Fuel Proc Technol 178:139–147. https://doi.org/10.1016/j.fuproc.2018.05.028

Lovell EC, Scott J, Amal R (2015) Ni–SiO_2 catalysts for the carbon dioxide reforming of methane: varying support properties by flame spray pyrolysis. Molecules 20:4594–4609. https://doi.org/10.3390/molecules20034594

Mandal V, Mohan Y, Hemalatha S (2007) Microwave assisted extraction-an innovative and promising extraction tool for medicinal plant research. Pharmacogn Rev 1(1):7–18

McMillan P, Partridge G (1972) The dielectric properties of certain ZnO–Al_2O_3–SiO_2 glass-ceramics. J Mater Sci 7:847–855. https://doi.org/10.1007/BF00550431

Meloni E, Martino M, Palma V (2020) A short review on Ni based catalysts and related engineering issues for methane steam reforming. Catalysts 10(3):352. https://doi.org/10.3390/catal10030352

Menéndez JA, Arenillas A, Fidalgo B, Fernández Y, Zubizarreta L, Calvo EG, Bermúdez JM (2010) Microwave heating processes involving carbon materials. Fuel Proc Technol 91:1–8. https://doi.org/10.1016/j.fuproc.2009.08.021

Meredith RJ (1998) Engineers' handbook of industrial microwave heating. IET, The Institution of Electrical Engineers, London

Metaxas AC, Meredith RJ (1983) Industrial microwave heating. IET, London

Mingos DMP, Baghurst DR (1991) Applications of microwave dielectric heating effects to synthetic problems in chemistry, microwave-enhanced chemistry. Chem Soc Rev 20:1–47. https://doi.org/10.1039/CS9912000001

Motasemi F, Afzal MT (2013) A review on the microwave-assisted pyrolysis technique. Renew Sustain Energy Rev 28:317–330. https://doi.org/10.1016/j.rser.2013.08.008

Muraza O, Galadima A (2015) A review on coke management during dry reforming of methane. Int J Energy Res 39(9):1196–1216. https://doi.org/10.1002/er.3295

Nematollahi B, Rezaei M, Lay EN, Khajenoori M (2012) Thermodynamic analysis of combined reforming process using Gibbs energy minimization method: in view of solid carbon formation. J Nat Gas Chem 21:694–702. https://doi.org/10.1016/S1003-9953(11)60421-0

Nguyen PHD, Le Nguyen KT, Nguyen TTN, Duong NL, Hoang TC, Pham TTP, Vo DVN (2019) Application of microwave-assisted technology: a green process to produce ginger products without waste. J Food Proc Eng 42:e12996. https://doi.org/10.1111/jfpe.12996

Nguyen HM, Sunarsoc J, Lia C, Pham GH, Phan C, Liu S (2020) Microwave-assisted catalytic methane reforming: a review. Appl Catal A Gen 599:117620. https://doi.org/10.1016/j.apcata.2020.117620

Nightingale S (2001) Interfacial phenomena in microwave sintering. Ionics 7:327–331. https://doi.org/10.1007/BF02373566

Nikoo MK, Amin NAS (2011) Thermodynamic analysis of carbon dioxide reforming of methane in view of solid carbon formation. Fuel Process Technol 92:678–691. https://doi.org/10.1016/j.fuproc.2010.11.027

Nüchter M, Ondruschka B, Bonrath W, Gum A (2004) Microwave assisted synthesis–a critical technology overview. Green Chem 6(3):128–141. https://doi.org/10.1039/B310502D

Odedairo T, Ma J, Chen J, Wang S, Zhu Z (2016) Influences of doping Cr/Fe/Ta on the performance of Ni/CeO_2 catalyst under microwave irradiation in dry reforming of CH_4. J Solid State Chem 233:166–177. https://doi.org/10.1016/j.jssc.2015.10.025

Ojeda-Niño OH, Gracia F, Daza C (2019) Role of Pr on Ni–Mg–Al mixed oxides synthesized by microwave-assisted self-combustion for dry reforming of methane. Ind Eng Chem Res 58:7909–7921. https://doi.org/10.1021/acs.iecr.9b00557

Pashchenko D (2017) Thermodynamic equilibrium analysis of combined dry and steam reforming of propane for thermochemical waste-heat recuperation. Int J Hydrog Energy 42:14926–14935. https://doi.org/10.1016/j.ijhydene.2017.04.284

Peng Z, Hwang JY, Kim BG, Mouris J, Hutcheon R (2012) Microwave absorption capability of high volatile bituminous coal during pyrolysis. Energy Fuels 26:5146–5151. https://doi.org/10.1021/ef300914f

Peng K, Zhou J, Xu W, You Z, Long W, Xiang M, Luo M (2017) Microwave irradiation-selective catalytic reduction of NO to N_2 by activated carbon at low temperature. Energy Fuels 31:7344–7351. https://doi.org/10.1021/acs.energyfuels.7b01102

Pham Minh D, Phan TS, Grouset D, Nzihou A (2018) Thermodynamic equilibrium study of methane reforming with carbon dioxide, water and oxygen. J Clean Energy Technol 6:309–313. https://doi.org/10.18178/JOCET.2018.6.4.480

Pham Minh D, Hernandez Torres A, Rego de Vasconcelos B, Siang TJ, Vo DVN (2020) Conversion of biogas to syngas via catalytic carbon dioxide reforming reactions: an overview of thermodynamic aspects, catalytic design, and reaction kinetics. In: Nanda S, Vo DVN, Sarangi PK (eds) Biorefinery of alternative resources: targeting green fuels and platform chemicals. Springer, Berlin, pp 427–456. https://doi.org/10.1007/978-981-15-1804-1_18

Protasov ON, Mamonov NA, Mikhailov MN, Kustov LM (2012) Optimization of equilibrium carbon dioxide methane reforming parameters by the gibbs free energy minimization method. Russ J Phys Chem A 86:741–746. https://doi.org/10.1134/S0036024412050305

Qin Z, Chen J, Xie X, Luo X, Su T, Ji H (2020) CO_2 reforming of CH_4 to syngas over nickel-based catalysts. Environ Chem Lett 18:1–21. https://doi.org/10.1007/s10311-020-00996-w

Qiu J, Qiu T (2015) Fabrication and microwave absorption properties of magnetite nanoparticle–carbon nanotube–hollow carbon fiber composites. Carbon 81:20–28. https://doi.org/10.1016/j.carbon.2014.09.011

Raje AP, Davis BH (1997) Fischer-Tropsch synthesis over iron-based catalysts in a slurry reactor. Reaction rates, selectivities and implications for improving hydrocarbon productivity. Catal Today 36(3):335–345. https://doi.org/10.1016/S0920-5861(96)00245-3

Razzaq T, Kappe CO (2008) On the energy efficiency of microwave-assisted organic reactions. Chemsuschem 1:123–132. https://doi.org/10.1002/cssc.200700036

Rodriguez-Reinoso F (1998) The role of carbon materials in heterogeneous catalysis. Carbon 36:159–175. https://doi.org/10.1016/S0008-6223(97)00173-5

Rosa R, Veronesi P, Casagrande A, Leonelli C (2016) Microwave ignition of the combustion synthesis of aluminides and field-related effects. J Alloys Compd 657:59–67. https://doi.org/10.1016/j.jallcom.2015.10.044

Rossi AS, Faria MG, Pereira MS, Ataíde CH (2017) Kinetics of microwave heating and drying of drilling fluids and drill cuttings. Dry Technol 35:1130–1140. https://doi.org/10.1080/07373937.2016.1233425

Roy R, Peelamedu R, Grimes C, Cheng J, Agrawal D (2002) Major phase transformations and magnetic property changes caused by electromagnetic fields at microwave frequencies. J Mater Res 17:3008–3011. https://doi.org/10.1557/JMR.2002.0437

Salema AA, Yeow YK, Ishaque K, Ani FN, Afzal MT, Hassan A (2013) Dielectric properties and microwave heating of oil palm biomass and biochar. Ind Crops Prod 50:366–374. https://doi.org/10.1016/j.indcrop.2013.08.007

Sarıyer M, Bozdağ AA, Sezgi NA, Doğu T (2019) Performance comparison of microwave and conventionally heated reactors for sorption enhanced reforming of ethanol over Ni impregnated SBA-15. Chem Eng J 377:120138. https://doi.org/10.1016/j.cej.2018.10.075

Schiffmann RF, Steiner R (2012) Inexpensive microwave leakage detectors-are they worth it? (A performance evaluation report). J Microw Power Electromagn Energy 46:128–138. https://doi.org/10.1080/08327823.2012.11689831

Shah YT, Gardner TH (2014) Dry reforming of hydrocarbon feedstocks. Catal Rev 56:476–536. https://doi.org/10.1080/01614940.2014.946848

Sheshko TF, Kryuchkova TA, Serov YM, Chislova IV, Zvereva IA (2017) New mixed perovskite-type $Gd_{2-x}Sr_{1+x}Fe_2O_7$ catalysts for dry reforming of methane, and production of light olefins. Catal Ind 9:162–169. https://doi.org/10.1134/S207005041702009X

Siang TJ, Singh S, Omoregbe O, Bach LG, Phuc NHH, Vo DVN (2018) Hydrogen production from CH_4 dry reforming over bimetallic Ni–Co/Al_2O_3 catalyst. J Energy Inst 91:683–694. https://doi.org/10.1016/j.joei.2017.06.001

Stefanidis GD, Munoz AN, Sturm GS, Stankiewicz A (2014) A helicopter view of microwave application to chemical processes: reactions, separations, and equipment concepts. Rev Chem Eng 30:233–259. https://doi.org/10.1515/revce-2013-0033

Sun J, Wang W, Yue Q (2016) Review on microwave-matter interaction fundamentals and efficient microwave-associated heating strategies. Materials 9:231. https://doi.org/10.3390/ma9040231

Thostenson ET, Chou TW (1999) Microwave processing: fundamentals and applications. Compos Part A Appl Sci Manuf 30:1055–1071. https://doi.org/10.1016/S1359-835X(99)00020-2

Tian S, Yan F, Zhang Z, Jiang J (2019) Calcium-looping reforming of methane realizes in situ CO_2 utilization with improved energy efficiency. Sci Adv 5:EAAV5077. https://doi.org/10.1126/sciadv.aav5077

Titirici MM, White RJ, Brun N, Budarin VL, Su DS, del Monte F, Clark JH, MacLachlan MJ (2015) Sustainable carbon materials. Chem Soc Rev 44:250–290. https://doi.org/10.1039/C4CS00232F

Tsang S, Claridge J, Green M (1995) Recent advances in the conversion of methane to synthesis gas. Catal Today 23(1):3–15. https://doi.org/10.1016/0920-5861(94)00080-L

Tu X, Whitehead JC (2012) Plasma-catalytic dry reforming of methane in an atmospheric dielectric barrier discharge: understanding the synergistic effect at low temperature. Appl Catal B Environ 125:439–448. https://doi.org/10.1016/j.apcatb.2012.06.006

Védrine JC (2005) Natural gas as feedstock. In: Derouane EG, Parmon V, Lemos F, Ramôa Ribeiro F (eds) Sustainable strategies for the upgrading of natural gas Fundamentals, challenges, and opportunities. NATO science series II: mathematics, physics and chemistry, vol 191. Springer, Dordrecht, pp 403–412

Verma P, Samanta SK (2018) Microwave-enhanced advanced oxidation processes for the degradation of dyes in water. Environ Chem Lett 16:969–1007. https://doi.org/10.1007/s10311-018-0739-2

Wang Y, Yao L, Wang S, Mao D, Hu C (2018) Low-temperature catalytic CO_2 dry reforming of methane on Ni-based catalysts: a review. Fuel Process Technol 169:199–206. https://doi.org/10.1016/j.fuproc.2017.10.007

Wang P, Liu PA, Ye S (2019) Preparation and microwave absorption properties of Ni(Co/Zn/Cu)Fe_2O_4/SiC@SiO_2 composites. Rare Met. https://doi.org/10.1007/s12598-016-0752-1

Wen F, Zhang F, Liu Z (2011) Investigation on microwave absorption properties for multiwalled carbon nanotubes/Fe/Co/Ni nanopowders as lightweight absorbers. J Phys Chem C 115:14025–14030. https://doi.org/10.1021/jp202078p

Westphal WB, Sils A (1972) Dielectric constant and loss data. Massachusetts Institute of Technology, Cambridge

Wiesbrock F, Hoogenboom R, Schubert US (2004) Microwave-assisted polymer synthesis: state-of-the-art and future perspectives. Macromol Rapid Commun 25:1739–1764. https://doi.org/10.1002/marc.200400313

Will H, Scholz P, Ondruschka B (2004) Microwave-assisted heterogeneous gas-phase catalysis. Chem Eng Technol 27:113–122. https://doi.org/10.1002/ceat.200401865

Xiong L, Yu M, Liu J, Li S, Xue B (2017) Preparation and evaluation of the microwave absorption properties of template-free graphene foam-supported Ni nanoparticles. RSC Adv 7:14733–14741. https://doi.org/10.1039/C6RA27435H

Xu W, Hu X, Xiang M, Luo M, Peng R, Lan L, Zhou J (2017a) Highly effective direct decomposition of H2S into H2 and S by microwave catalysis over CoS-MoS_2/γ-Al_2O_3 microwave catalysts. Chem Eng J 326:1020–1029. https://doi.org/10.1016/j.cej.2017.06.027

Xu W, Luo M, Peng R, Xiang M, Hu X, Lan L, Zhou J (2017b) Highly effective microwave catalytic direct decomposition of H_2S into H_2 and S over MeS-based (Me = Ni, Co) microwave catalysts. Energy Conver Manag 149:219–227. https://doi.org/10.1016/j.enconman.2017.07.029

Xu Y, Du XH, Li J, Wang P, Zhu J, Ge FJ, Zhou J, Song M, Zhu WY (2019) A comparison of Al_2O_3 and SiO_2 supported Ni-based catalysts in their performance for the dry reforming of methane. J Fuel Chem Technol 47:199–208. https://doi.org/10.1016/S1872-5813(19)30010-6

Yin P, Deng Y, Zhang L, Li N, Feng X, Wang J, Zhang Y (2018) Facile synthesis and microwave absorption investigation of activated carbon@Fe_3O_4 composites in the low frequency band. RSC Adv 8:23048–23057. https://doi.org/10.1039/C8RA04141E

York AP, Xiao T, Green ML (2003) Brief overview of the partial oxidation of methane to synthesis gas. Top Catal 22(3–4):345–358. https://doi.org/10.1023/A:1023552709642

Yoshikawa N, Ishizuka E, Taniguchi S (2006) Heating of metal particles in a single-mode microwave applicator. Mater Trans 47:898–902. https://doi.org/10.2320/matertrans.47.898

Zhang X, Hayward DO (2006) Applications of microwave dielectric heating in environment-related heterogeneous gas-phase catalytic systems. Inorg Chim Acta 359:3421–3433. https://doi.org/10.1016/j.ica.2006.01.037

Zhang X, Hayward DO, Mingos DMP (1999) Apparent equilibrium shifts and hot-spot formation for catalytic reactions induced by microwave dielectric heating. Chem Commun. https://doi.org/10.1039/A901245A

Zhang X, Hayward DO, Lee C, Mingos DMP (2001) Microwave assisted catalytic reduction of sulfur dioxide with methane over MoS_2 catalysts. Appl Catal B Environ 33:137–148. https://doi.org/10.1016/S0926-3373(01)00171-0

Zhang X, Hayward DO, Mingos DMP (2002) Dielectric properties of MoS_2 and Pt catalysts: effects of temperature and microwave frequency. Catal Lett 84(3–4):225–233. https://doi.org/10.1023/A:1021488222243

Zhang X, Lee CSM, Mingos DMP, Hayward DO (2003) Carbon dioxide reforming of methane with Pt catalysts using microwave dielectric heating. Catal Lett 88:129–139. https://doi.org/10.1023/A:1024049403422

Zhang Y, Zhang S, Zhang X, Qiu J, Yu L, Shi C (2015) Ni modified WCx catalysts for methane dry reforming. In: Jin F, He LN, Hu YH (eds) Advances in CO2 capture, sequestration, and conversion, vol 1194. American Chemical Society, Washington, pp 171–189. https://doi.org/10.1021/bk-2015-1194.ch008

Zhang F, Song Z, Zhu J, Liu L, Sun J, Zhao X, Mao Y, Wang W (2018a) Process of CH_4–CO_2 reforming over Fe/SiC catalyst under microwave irradiation. Sci Total Environ 639:1148–1155. https://doi.org/10.1016/j.scitotenv.2018.04.364

Zhang F, Song Z, Zhu J, Sun J, Zhao X, Mao Y, Liu L, Wang W (2018b) Factors influencing CH_4–CO_2 reforming reaction over Fe catalyst supported on foam ceramics under microwave irradiation. Int J Hydrog Energy 43:9495–9502. https://doi.org/10.1016/j.ijhydene.2018.03.171

Zhang YJ, Wang ZJ, Chen YN, Zhang ZD (2018c) Crystallization kinetics of $PbTiO_3$ ferroelectric films: comparison of microwave irradiation with conventional heating. J Eur Ceram Soc 38:105–111. https://doi.org/10.1016/j.jeurceramsoc.2017.08.030

Zhao B, Shao G, Fan B, Zhao W, Chen Y, Zhang R (2015) Facile synthesis of crumpled ZnS net-wrapped Ni walnut spheres with enhanced microwave absorption properties. RSC Adv 5:9806–9814. https://doi.org/10.1039/C4RA15411H

Zhu YJ, Chen F (2014) Microwave-assisted preparation of inorganic nanostructures in liquid phase. Chem Rev 114:6462–6555. https://doi.org/10.1021/cr400366s

Zhu H, He J, Yang Q, Yang Y, Huang K (2017) A rotary radiation structure of microwave reactor for advanced materials processing. In: 2017 international conference on information, communication and engineering (ICICE), pp 404–407

Zlotorzynski A (1995) The application of microwave radiation to analytical and environmental chemistry. Crit Rev Anal Chem 25:43–76. https://doi.org/10.1080/10408349508050557